Geological Magazine

www.cambridge.org/geo

A Palaeoarchean–Mesoarchean micro-continent entrained in the Jiao-Liao-Ji Belt at the southeastern North China Craton: evidence from the zircon record in the Bengbu area

Chaohui Liu[1], Guochun Zhao[2], Fulai Liu[1] and Jia Cai[1]

[1]Institute of Geology, Chinese Academy of Geological Sciences, Beijing 100037, China and [2]Department of Earth Sciences, University of Hong Kong, Pokfulam Road, Hong Kong

Original Article

Cite this article: Liu C, Zhao G, Liu F, and Cai J. (2019) A Palaeoarchean–Mesoarchean micro-continent entrained in the Jiao-Liao-Ji Belt at the southeastern North China Craton: evidence from the zircon record in the Bengbu area. *Geological Magazine* **156**: 1565–1586. https://doi.org/10.1017/S0016756818000869

Received: 3 April 2018
Revised: 25 September 2018
Accepted: 17 November 2018
First published online: 18 March 2019

Keywords:
Bengbu area; Jiao-Liao-Ji Belt; North China Craton; Palaeoarchean–Palaeoproterozoic; zirconology

Author for correspondence: Chaohui Liu, Email: denverliu82@gmail.com

Abstract

The Bengbu area in the southeastern North China Craton (NCC) consists predominantly of Archean–Palaeoproterozoic (gneissic) granitoids with minor supracrustal rocks (the Fengyang and Wuhe groups). This study presents new zircon laser ablation – inductively coupled plasma – mass spectrometry U–Pb and Lu–Hf isotopic data and trace-element contents for these granitoids, which improve understanding the Archean–Palaeoproterozoic crustal evolution of the NCC. Magmatic zircon U–Pb data reveal that zircons in the (gneissic) granitoids were generated by multi-stage events at 2.93, 2.73, 2.53–2.52 and 2.18–2.13 Ga. Metamorphic zircon U–Pb data obtained from these rocks show two distinct metamorphic ages of 2.49–2.52 and 1.84 Ga, suggesting that the Bengbu area experienced a regional metamorphic event at the end of the Neoarchean Era and encountered reworking by a tectonothermal event associated with the formation of the Palaeoproterozoic Jiao-Liao-Ji Belt. Trace-element compositions of magmatic zircons reveal the highest Ti concentrations (8.08±3.38 ppm) and growth temperatures (718±44 °C) for the zircons aged 2.13–2.17 Ga and an increase in zircon U/Yb ratios from 2.93 Ga (0.34±0.12) through 2.73 Ga (0.96±0.42) to 2.53 Ga (1.05±0.46), but an evident decrease at 2.17–2.13 Ga (0.61±0.40 ppm). Similar Palaeoarchean xenocrystic and detrital zircons with negative $\varepsilon_{Hf}(t)$ values, late Mesoarchean magmatic zircons with juvenile Hf isotopic features, early Neoarchean magmatic zircons with model ages of 2.9–3.0 Ga, and two regional metamorphic events at 2.52–2.48 and 1.88–1.80 Ga in the Bengbu and Jiaobei areas indicate a Palaeoarchean–Mesoarchean micro-continent entrained in the Jiao-Liao-Ji Belt at the southeastern NCC.

1. Introduction

The North China Craton (NCC) is one of the few areas on Earth where rocks older than 3.8 Ga have been identified (Liu *et al.* 1992; Song *et al.* 1996; Wan *et al.* 2005) and rocks older than *c.* 2.6 Ga occur widely (Wan *et al.* 2015). The Archean crustal growth and reworking, the tectonic subdivision and amalgamation, the major magmatic and metamorphic events, and the tectonic settings of the NCC have attracted much attention within the international geological community in the past decades (Bai & Dai, 1996; Wu *et al.* 1998; Zhao *et al.* 2005; Lu *et al.* 2008; Zhai *et al.* 2000, 2005, 2010; Nutman *et al.* 2011; Zhai & Santosh, 2011; Zhang *et al.* 2012; Wang *et al.* 2015; Liu *et al.* 2017*a*). As the most voluminous rock type in Archean–Palaeoproterozoic cratonic blocks, the tonalite-trondhjemite-granodiorite (TTG) and potassium-rich granite gneisses (Barker, 1979) are widely distributed in the preserved basement of the NCC, providing an opportunity to constrain the crustal growth, recycling, metamorphism and their tectonic settings. However, several events since the late Palaeoproterozoic Era modified the original features of the basement and make it difficult to comprehensively understand the early Precambrian geology of the NCC, so significant debates are still ongoing as indicated by different tectonic models, especially for the Neoarchean granitic gneisses and associated rocks in the eastern NCC (Geng *et al.* 2006; Tang *et al.* 2007; Jahn *et al.* 2008; Yang *et al.* 2008; Nutman *et al.* 2011; Wan *et al.* 2014; Xie *et al.* 2014*a*; Shan *et al.* 2015; Wang *et al.* 2015).

Zircon is an accessory mineral in a wide variety of igneous rocks (especially intermediate to felsic intrusive rocks), and is one of the most useful minerals for gaining detailed information about the formation, recycling and metamorphism of high-grade gneiss terranes (Zheng *et al.* 2006; Wu *et al.* 2008; Gerdes & Zeh, 2009; Liu *et al.* 2010*a*; Zeh *et al.* 2010; Heinonen *et al.* 2015; Mukherjee *et al.* 2017) because of its resistance to recrystallization during hydrothermal alteration. As well as internal zoning patterns (Corfu *et al.* 2003; Harley *et al.* 2007), U–Th–Pb and Lu–Hf isotopes provide information about magmatic and/or metamorphic events and crustal evolution (Amelin *et al.* 1999, 2000; Kinny & Maas, 2003; Griffin *et al.* 2004; Hawkesworth & Kemp, 2006; Wu *et al.* 2007), and the minor- and trace-element geochemistry of zircon is an indicator of its parental magma composition (Hoskin & Schaltegger, 2003; Hoskin, 2005).

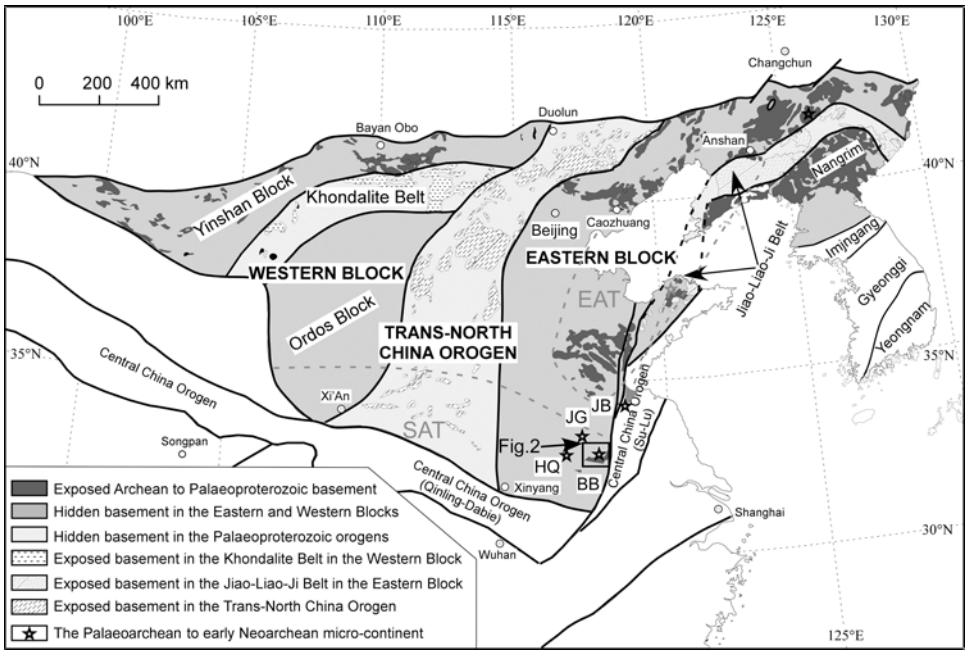

Fig. 1. Tectonic subdivision of the North China Craton (modified after Zhao *et al.* 2005), showing the distribution of the Eastern Ancient Terrane (EAT) and Southern Ancient Terrane (SAT; Wan *et al.* 2015). Note that the cropped out rocks or xenocrystic zircons with Palaeoarchean – early Neoarchean ages are indicated by stars. The early Precambrian position of the Jiaobei Terrane is based on the *c.* 400 km offset along the Mesozoic NE-striking Tan-Lu Fault (Zhao *et al.* 2016). JG – Jiagou; JB – Jiaobei; HQ – Huoqiu; BB – Bengbu.

Additionally, using an analytically consistent set of zircon trace-element data (including U, Yb, Nb, Sc, Ce and Gd), it is possible to discriminate the tectonomagmatic settings of mid-ocean ridge, plume-influenced ocean island and subduction-related arc environments (Grimes *et al.* 2007, 2015; Carley *et al.* 2014).

Different models have been proposed for the tectonic subdivision of the NCC since the application of terrane accretion and collision models (Wu *et al.* 1998; Zhao *et al.* 1998; Zhai *et al.* 2000; Kusky & Li, 2003; Faure *et al.* 2007; Kusky *et al.* 2007; Santosh, 2010; Wan *et al.* 2015). In the southeastern NCC, the Bengbu area has been suggested as belonging to the Yuwan Block (Wu *et al.* 1998), the Xuhuai Block (Zhai *et al.* 2011) and the Eastern Block (Zhao *et al.* 2005). More recently, Wan *et al.* (2015) delineated three Archean terranes based on the spatial distribution of ancient rocks and zircons, namely the Eastern, Southern and Central ancient terranes (Fig. 1), in which the Bengbu area is located in the eastern end of the Southern Ancient Terrane and is suggested to be comparable with the Xinyang, Lushan, Huoqiu and Zhongtiao areas based on occurrences of zircons or rocks of age 3.65, 2.82–2.83 and 2.6–2.7 Ga (Wan *et al.* 2017). However, recent geochronological studies in the Huoqiu area suggest two magmatic events at 2.76–2.71 Ga (Wan *et al.* 2010; Yang *et al.* 2012; Wang *et al.* 2014*a*) and 2.56–2.48 Ga (Wan *et al.* 2010; Wang *et al.* 2012*a*; Liu *et al.* 2013*a*), and xenocrystic zircons of age 2.90–2.95 Ga have also been found (Yang *et al.* 2012; Liu *et al.* 2015*a*). In the Palaeoproterozoic Fengyang and Wuhe groups in the Bengbu area, the Archean detrital zircons yield similar age peaks of 2.88–2.94, 2.69–2.77 and 2.52–2.55 Ga (Liu & Cai, 2017; Liu *et al.* 2018). Additionally, in consideration of an *c.* 400 km offset along the Mesozoic NE-striking Tan-Lu Fault (Zhao *et al.* 2016; Fig. 1), the Jiaobei Terrane assigned to the East Ancient Terrane (Wan *et al.* 2015) has a close spatial relationship with the Bengbu area and also underwent three episodes of magmatic events at 2.93–2.86, 2.74–2.69 and 2.56–2.50 Ga (Faure *et al.* 2003; Tang *et al.* 2004, 2007; Jahn *et al.* 2008; Zhou *et al.* 2008*a*; Liu *et al.* 2013*b*; Xie *et al.* 2013, 2014*a*, 2015; Wang *et al.* 2014*b*; Wu *et al.* 2014*a*; Zhang *et al.* 2014; Shan *et al.* 2015). However, it is still uncertain whether the Huoqiu, Bengbu and Jiaobei areas shared the same formation and evolution processes during the Archean–Palaeoproterozoic period. In this study, *in situ* zircon Th–U–Pb and Lu–Hf isotopes and trace-element compositions were analysed using laser ablation – multi-collector – inductively coupled plasma – mass spectrometry (LA-(MC)-ICP-MS) applied to eight early Palaeoproterozoic – Archean granitoids in the Bengbu area, with a view to (1) determining their formation and metamorphic ages; (2) comparing the crust growth and reworking history of the Huoqiu, Bengbu and Jiaobei areas; and (3) providing evidence for a Palaeo- to Mesoarchean micro-continent entrained in the Jiao-Liao-Ji Belt at the southeastern NCC.

2. Regional geology

In the last decades, three Palaeoproterozoic mobile belts – the Khondalite Belt, the Trans-North China Orogen and the Jiao-Liao-Ji Belt (JLJB) (Zhao *et al.* 2005, 2012), alternatively named the Fengzhen, Jinyu and Liaoji belts (Zhai & Peng, 2007; Zhai & Santosh, 2011), have been identified in the NCC. The Trans-North China Orogen divides the NCC into the Western Block and Eastern Block, and the Khondalite Belt subdivides the Western Block into the Yinshan Block in the north and the Ordos Block in the south (Fig. 1; Zhao *et al.* 2005, 2012). Previous studies suggested that the Yinshan and Ordos blocks collided along the Khondalite Belt at *c.* 1.95 Ga (Yin *et al.* 2011, 2014; Wan *et al.* 2013), and then the consolidated Western Block amalgamated with the Eastern Block along the Trans-North China Orogen at *c.* 1.85 Ga (Zhao *et al.* 2005, 2012) or slightly earlier at 1.95 Ga (Zhang *et al.* 2013; Qian & Wei 2016).

The nearly N–S-trending JLJB is located in the eastern part of the Eastern Block and extends for *c.* 1200 km from southern Jilin,

https://doi.org/10.1017/S0016756818000869 Published online by Cambridge University Press

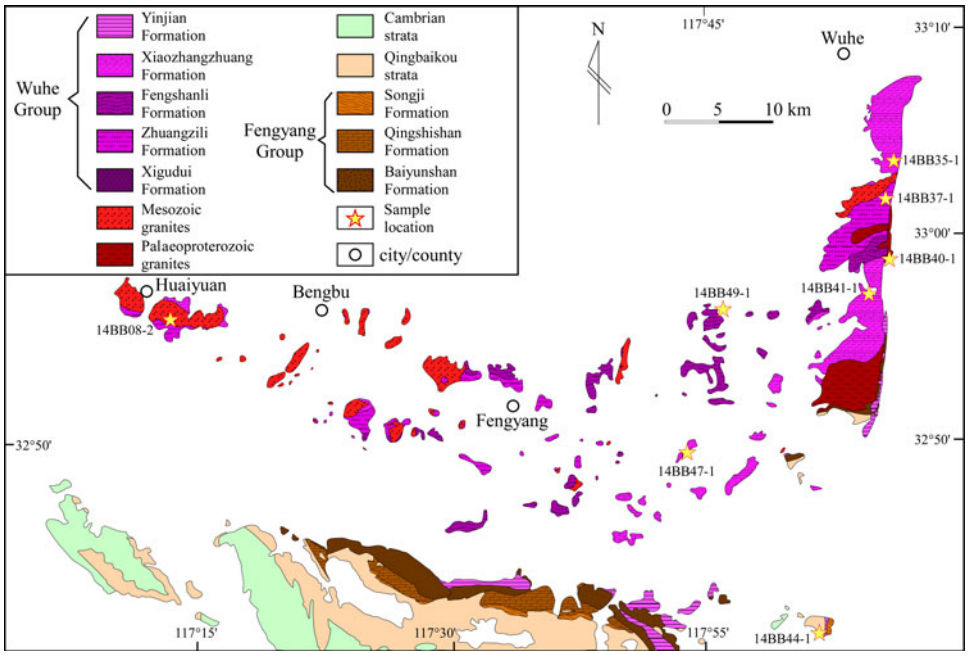

Fig. 2. (Colour online) Distributions of Precambrian basement rocks and sedimentary cover in the Bengbu area (modified after Liu *et al.* 2015*c*).

through the Liaodong Peninsula and into the Jiaodong Peninsula (Fig. 1). Previous geochronological studies in the belt showed that most of the supracrustal successions and pre-tectonic granitoids formed during 2.20–2.10 Ga and were metamorphosed and deformed during 1.95–1.90 Ga (Luo *et al.* 2004, 2008; Li *et al.* 2005; Lu *et al.* 2006, 2004; Li & Zhao, 2007; Zhou *et al.* 2008*b*; Tam *et al.* 2011; Liu *et al.* 2012*a*, 2013*c*), whereas the post-tectonic granites were emplaced at 1.88–1.83 Ga (Hao *et al.* 2004; Lu *et al.* 2006; Li & Zhao, 2007; Liu *et al.* 2017*b*).

The Jiaobei Terrane, considered as the south segment of the JLJB (Zhao *et al.* 2005), is bounded by the Tan-Lu Fault to the NW and the Wulian-Yantai Fault to the SE, the latter being commonly regarded as the boundary between the NCC and South China Craton (Wallis *et al.* 1999; Tang *et al.* 2007; Zhang *et al.* 2014). The Precambrian metamorphic basement is mainly composed of Archean–Palaeoproterozoic supracrustal rocks and (gneissic) granitoids (SBGMR, 1991; Lu, 1998; Zhou *et al.* 2004, 2008*a*, *b*; Tang *et al.* 2007; Jahn *et al.* 2008; Tam *et al.* 2012). The Archean supracrustal rocks, which occur sparsely within TTG gneisses, are mainly biotite-plagioclase gneiss, biotite leptite, leuco-leptite, amphibolite and banded iron formation (BIF), all of which underwent amphibolite- to granulite-facies metamorphism. Amphibole ^{39}Ar–^{40}Ar and zircon U–Pb geochronological studies showed that they formed at *c.* 2.89 Ga (Jahn *et al.* 2008) and experienced two episodes of metamorphism at 2.52–2.45 and 1.96–1.79 Ga (Faure *et al.* 2003; Tang *et al.* 2007; Jahn *et al.* 2008; Zhou *et al.* 2008*b*; Tam *et al.* 2011; Liu *et al.* 2012*a*; Xie *et al.* 2013; Wang *et al.* 2014*b*; Wu *et al.* 2014*a*). The Palaeoproterozoic Fenzishan and Jingshan groups unconformably overlie the Archean TTG gneisses, and are composed mainly of Al-rich sillimanite-garnet-biotite-quartz schist, biotite leptite and gneiss, felsic paragneiss, marble and amphibolite. Metamorphic zircon ages of 1.80–1.95 Ga (Wan *et al.* 2006; Zhou *et al.* 2008*b*; Wang *et al.* 2010; Tam *et al.* 2011; Zhang *et al.* 2014) and detrital zircon ages of 2.00–3.40 Ga with peaks at 2.10–2.20 and 2.45–2.50 Ga (Wan *et al.* 2006; Xie *et al.* 2014*b*; Liu *et al.* 2015*b*) have been reported. The Archean granitoid (TTG and potassium granite) gneisses are mainly exposed in the Qixia area and are characterized by ductile shear deformation and anatexis resulting from amphibolite- to granulite-facies metamorphism (Liu *et al.* 2012*a*, 2013*c*; Tam *et al.* 2011). Zircon U-Pb dating results gave protolith ages of 2.86–2.93 Ga, 2.69–2.74 Ga and 2.50–2.56 Ga and metamorphism/anatexis ages of 2.46–2.52 Ga and 1.86–1.90 Ga for the TTG gneisses (Tang *et al.* 2004, 2007; Jahn *et al.* 2008; Zhou *et al.* 2008*a*, *b*; Liu *et al.* 2012*a*, 2013*b*, *c*; Xie *et al.* 2013, 2014*a*, 2015; Wang *et al.* 2014*b*; Wu *et al.* 2014*a*; Shan *et al.* 2015). TTG gneisses are intruded by Palaeoproterozoic granitoids and mafic intrusions in the north of the Qixia, of which the former consists of deformed or undeformed monzogranites and granites, and the latter consists of gabbros and dolerites forming walls or sheets in the granitoid plutons. Relatively little work has been undertaken on these granitoid rocks and gabbros, and only two stages of zircon U–Pb ages of 2.10–2.18 and 1.80–1.84 Ga have been obtained (Liu *et al.* 2014; Wang *et al.* 2014*b*).

The Precambrian basements at the southeastern margin of the NCC are distributed in the Huoqiu and Bengbu areas, which lie about 70 km west of the Tan-Lu fault zone (Fig. 1) and were suggested as the southwestern extension of the JLJB (Zhao *et al.* 2012; Wang *et al.* 2017*a*; Liu *et al.* 2018). In the Huoqiu area, the basement rocks are covered by late Precambrian and Quaternary strata and are composed of meta-supracrustal rocks and granitoid intrusions based on the drilling data (Yang *et al.* 2012; Wang *et al.* 2014*a*). Recent LA-ICP-MS and secondary ion mass spectrometry (SIMS) zircon dating results suggested that the plagioclase amphibolite formed at 2.71 Ga with xenocrystic zircons of 2.95 Ga (Yang *et al.* 2012). The metamorphosed siliciclastic rocks have two age groups at 2.95–3.02 and 2.74–2.77 Ga (Wan *et al.* 2010, Wang *et al.* 2014*a*; Liu *et al.* 2015*a*) and the granitoids emplaced at 2.76–2.71, 2.56 and 1.92–1.82 Ga (Wan *et al.* 2010; Yang *et al.* 2012; Wang *et al.* 2014*a*; Liu *et al.* 2015*a*, 2016; Liu & Yang, 2015). Additionally, metamorphic zircons of 2.44 and 1.82 Ga have also been reported (Wan *et al.* 2010; Liu *et al.* 2015*a*).

In the Bengbu area, the previously reported metamorphosed granitoids include the Palaeoproterozoic Zhuangzili and Shimenshan

https://doi.org/10.1017/S0016756818000869 Published online by Cambridge University Press

plutons (Fig. 2; Guo & Li, 2009; Yang *et al.* 2009), whose deformation and emplacement ages are constrained at 2.06–2.10 Ga (Guo & Li, 2009; Yang *et al.* 2009; Wang *et al.* 2017*a*) and 1.74 Ga (Xu *et al.* 2005), respectively. Based on the A-type granite geochemical feature, the high whole-rock $\varepsilon_{Nd}(t)$ values and zircon $\varepsilon_{Hf}(t)$ values, and the presence of inherited zircons of age *c.* 2.48 Ga, these potassic granites were suggested to derived from partial melting of TTG gneisses and juvenile mafic crust material at *c.* 2.5 Ga at an extensional tectonic setting (Yang *et al.* 2009; Wang *et al.* 2017*a*).

The supracrustal successions in the Bengbu area have been divided into the Wuhe and Fengyang groups (ABGMR, 1987). The Wuhe Group, which is composed chiefly of greenschist- to granulite-facies metamorphosed flysch-type sedimentary and volcanic rocks, has been subdivided into two subgroups separated by a disconformity (ABGMR, 1987). Tu et al. (1992) reported a muscovite K–Ar age of 1.65 Ga in the Yinjian Formation of the upper subgroup and suggested that the formation should be removed from the group. However, the youngest group of detrital zircons from a muscovite-quartz schist of the formation yielded ages of 2.16–2.19 Ga, consistent with the crystallization age of 2.13 Ga of a plagioclase amphibolite and the youngest detrital zircon group of 2.15–2.17 Ga from the lower group (Liu *et al.* 2018). On the other hand, metamorphic and anatectic zircons of age 1.8–1.9 Ga have been found in the lower subgroup, and metamorphic studies implied that the meta-mafic rocks and marbles experienced high-pressure granulite-facies metamorphism at 1.9–1.8 Ga (Xu *et al.* 2006; Guo & Li, 2009; Liu *et al.* 2009, 2017*c*, 2018; Wang *et al.* 2013).

The low greenschist-facies metamorphosed Fengyang Group is mainly confined to a 30-km long E–W-trending belt in the southern Bengbu area (Fig. 2) and is composed of metamorphosed sandstones, siltstones, mudstones, Mg-rich carbonates and marlaceous rocks (ABGMR, 1987). Detrital zircon U–Pb dating results from the quartzites of the lowest formation gave the major age peak of *c.* 2.52 Ga, the minor age peaks of *c.* 2.94 and *c.* 2.69 Ga, and the youngest age group of *c.* 2.37 Ga (Liu & Cai, 2017). In consideration of similar detrital zircon age patterns and Lu–Hf isotopic features with those from the Huoqiu and Bengbu areas, Liu & Cai (2017) suggested that the early–late Neoarchean granitic rocks and the proximal metamorphosed supracrustal rocks are the main source rocks for the group.

As well as the early Precambrian metamorphic basement exposure, abundant Neoarchean–Palaeoproterozoic mantle and lower crustal xenoliths have been found in the Mesozoic dioritic porphyries in the southeastern NCC. Most of the xenoliths are basic to intermediate composition and include garnet-plagioclase amphibolite, garnet amphibolite, garnet granulite, garnet-bearing plagioclase-amphibole gneiss and granitic gneiss (Liu *et al.* 2015*c*). Previous zircon U–Pb dating results suggest that these xenoliths record two stages of magmatism at 2.55–2.48 and 2.12 Ga and two stages of metamorphism at 2.49–2.47 and 1.90–1.80 Ga (Huang *et al.* 2004; Xu *et al.* 2006; Guo & Li, 2009; Liu *et al.* 2009, 2013*b*; Wang *et al.* 2012*a*).

3. Analytical methods

Fresh portions of eight representative granitic samples were crushed to *c.* 40–80 mesh and zircon grains were separated using a combination of density and magnetic techniques. Selected grains were then mounted in epoxy resin and polished to approximately half-grain thickness. After reflected and transmitted light photographing, cathodoluminescence (CL) imaging was taken by a JSM6510 scanning electron microscope (SEM) attached with a Gatan CL detector. Zircon U–Pb isotopic analysis were conducted on the transparent grains without obvious fracture or mineral inclusion using an Agilent 7700× ICP-MS at Nanjing FocuMS Technology Co. Ltd. The mounted grains were ablated using an attached Analyte Excite laser-ablation system with a spot diameter of 35 μm at 8 Hz repetition rate for 40 seconds (equivalent to 320 pulses). Ablation occurred in intervals of eight sample zircons, directly preceded and followed by two zircon 91500 crystals as external standard and one zircon GJ-1 crystal as quality control. ICPMSDataCal software 8.0 (Liu *et al.* 2010*b*) was used to select off-line raw data, integrate background and analytical signals, correct for time-drift, and quantitatively calibrate U–Pb isotopes and trace-element concentrations. Possible mixing of different age domains due to the relatively deep ablation depth (35 μm) and complexly zoned zircons was avoided by not choosing later-stage analytical signals with obviously changed $^{207}Pb/^{206}Pb$ ratios. Common lead correction was conducted following the method of Anderson (2002). Concordia diagram plotting, probability density plotting and weighted average age calculation were carried out using Isoplot/Ex_ver 3.27 (Ludwig, 2003).

For the youngest group of igneous grains with concordant ages large enough to accommodate another laser ablation spot, trace elements were measured using the same grain mount and the same LA-ICP-MS instrument in an effort to fingerprint their source reservoirs. NIST 612 was used as an external standard and analysis spots were undertaken on the same CL domain and as closely as possible to the U–Pb analysis spots. Samples and reference materials were analysed for 30 isotopes: ^{29}Si, ^{31}P, ^{39}K, ^{42}Ca, ^{49}Ti, ^{85}Rb, ^{88}Sr, ^{89}Y, ^{91}Zr, ^{93}Nb, ^{139}La, ^{140}Ce, ^{141}Pr, ^{146}Nd, ^{147}Sm, ^{153}Eu, ^{157}Gd, ^{159}Tb, ^{163}Dy, ^{165}Ho, ^{166}Er, ^{169}Tm, ^{172}Yb, ^{175}Lu, ^{178}Hf, ^{181}Ta, ^{202}Hg, ^{204}Pb, ^{232}Th and ^{238}U. Corrections were made for mass bias drift which was evaluated by reference to standard glass NIST 610, and trace-element concentrations were obtained by normalizing count rates for each analysed element to those for Si, and assuming SiO_2 to be stoichiometric in zircon with a concentration of *c.* 32.8 wt%. P, Ca, Ti and Th were used in this study to evaluate possible involvements of mineral inclusions (apatite, titanite, feldspar and monazite) in the studied zircons; when evident spikes of these elements were encountered, the analysis was discarded. To check for reproducibility, precision and accuracy, NIST 612 glass was also analysed after certain NIST 610 analysis as reference material for trace elements, and cross-calibration between NIST 610 and NIST 612 was conducted. Most trace-element concentrations measured for NIST 610 relative to NIST 612 agree within error with published data and vice versa, indicating that our technique is accurate.

Zircon Lu–Hf isotopic ratio analyses were conducted following U–Pb and trace-element analyses of the relatively large zircon grains with concordant U–Pb ages. Lu–Hf analysis spots were undertaken on the same CL domain and as closely as possible to the U–Pb analysis spots. Teledyne Cetac Technologies Analyte Excite laser-ablation system and Nu Plasma II MC-ICP-MS were combined for the experiments at Nanjing FocuMS Co. Ltd. Ablation protocol used a spot diameter of 50 μm at 8 Hz repetition rate for 40 seconds (equivalent to 320 pulses). Possible mixing of different age domains due to the relatively deep ablation depth (50 μm) and complexly zoned zircons was avoided by not choosing later-stage analytical signals with obviously changed $^{176}Hf/^{177}Hf$ ratios. Zircon GJ-1 was used as the reference standard and gave a weighted average $^{176}Hf/^{177}Hf$ ratio of 0.282011±0.000004 (2σ, n=22), indistinguishable from the ratio of 0.282000±0.000005

https://doi.org/10.1017/S0016756818000869 Published online by Cambridge University Press

(2σ) by solution analysis method (Morel *et al.* 2008). ε_{Hf} values were calculated based on the present-day chondritic $^{176}Hf/^{177}Hf$ ratio of 0.282772 and $^{176}Lu/^{177}Hf$ ratio of 0.0332 (Blichert-Toft and Albarede, 1997).

4. Results

4.a. Zircon U–Pb geochronology

We present zircon U–Pb ages for five granitic samples and three granitic gneiss samples in the Bengbu area (Table 1). All analytical data are presented in online Supplementary Table S1 (available at http://journals.cambridge.org/geo).

A Mesoarchean granodioritic gneiss sample (14BB44-1) was collected from a roadside outcrop *c.* 8 km SE of Hongxin Town (32.65828° N, 117.87200° E; Fig. 2). Dark biotite leptite, heavily weathered, occurred as enclaves in the gneiss, both of which were weakly mylonitized (Fig. 3a). Major phases of the sample were plagioclase (45%) and quartz (45%), with minor amounts of biotite, hornblende and K-feldspar; some biotite and hornblende were retrogressed to chlorite and some plagioclase were altered to muscovite (Fig. 4a). Zircon grains were 100–150 μm in length with length/width ratios of 1:1–2.5:1 (Fig. 5). CL images revealed bright oscillatory zoning patterns without an obvious core–rim structure. A total of 30 analyses were performed on 30 grains, yielding apparent $^{207}Pb/^{206}Pb$ ages of 2909–2947 Ma (Fig. 6a) which form the upper intercept age of 2934±6 Ma (MSWD=0.53), consistent with the weighted mean age of 2929±7 Ma (MSWD=0.33) defined by the 23 concordant analyses (Fig. 6a). These analyses are characterized by high Th/U ratios of 0.50–1.74 (Fig. 7d), low light rare earth element (LREE) and high heavy rare earth element (HREE) patterns with negative Eu anomalies (median Eu/Eu* = 0.41) and obvious positive Ce anomalies (median Ce/Ce* = 7.63; Fig. 8a). Based on these features, the weighted mean age of 2929±7 Ma is interpreted as the crystallization age of the magmatic precursor of the granodioritic gneiss.

An early Neoarchean granodioritic gneiss sample (14BB35-1) was taken from a locality *c.* 10 km SE of Wuhe County (33.06038° N, 117.93361° E; Fig. 2), which is intruded by a Mesozoic dark hornblende granite (our unpublished data; Fig. 3b). The investigated sample was composed of quartz (30%), plagioclase (40%), (carbonatized) K-feldspar (10%), biotite (5%) and hornblende (5%), with minor amounts of apatite and zircon (Fig. 4b). Zircon grains were smaller than those from the Mesoarchean sample, being 80–100 μm in length with length/width ratios of 1:1–2:1 (Fig. 5). CL images revealed variably eroded oscillatory zoned or dark structureless cores enveloped by bright to dullish rims. A total of 60 analyses were conducted on 55 zircon grains, of which 55 older analyses with apparent $^{207}Pb/^{206}Pb$ ages of 2702–2918 Ma on the oscillatory zoned cores could be subdivided into three groups on the probability density plot (Fig. 6b). The oldest group was composed of two analyses, which had Th/U ratios of 0.34 and 0.65 and apparent ages of 2905 and 2918 Ma (Supplementary Table S1; Fig. 6b). The second group was composed of 32 analyses, with Th/U ratios of 0.14–0.98 (Supplementary Table S1). These data showed apparent ages of 2802–2860 Ma and yielded the upper intercept age of 2831±10 Ma (MSWD=1.6), consistent with the weighted mean age (2829±7 Ma) of the concordant analyses (Fig. 6b). The third group consisted of 21 analyses, which showed apparent ages and Th/U ratios of 2694–2759 Ma and 0.17–0.63, respectively (Supplementary Table S1). They yielded the upper intercept age of 2729±14 Ma (MSWD=1.5), consistent with the weighted mean age (2731±9 Ma) of the concordant analyses (Fig. 6b). On the other hand, five analyses conducted on the bright rims had relatively lower Th/U ratio than those on the cores, and gave apparent ages of 2502–2540 Ma (Supplementary Table S1), yielding an upper intercept age of 2517±40 Ma (MSWD=0.41) and a weighted mean age of 2524±41 Ma (MSWD=0.38; Fig. 6b). Based on the zircon internal structures, the magmatic precursor is considered to have been emplaced at 2731±9 Ma and subjected to later (*c.* 2524 Ma) metamorphism.

A late Neoarchean medium-grained monzogranitic gneiss (sample 14BB41-1) was collected from a roadside outcrop in the south of Wuhe County (32.95094° N, 117.91032° E; Fig. 2). The gneiss had a mineral assemblage of quartz (45%), plagioclase (20%), K-feldspar (15%), muscovite (10%) and tourmaline (5%; Fig. 4c). Zircon grains from this sample were relatively large with lengths and length/width ratios of 150–200 μm and 1:1–2:1, respectively (Fig. 5). CL images revealed blurred oscillatory zoned or structureless cores enveloped by clearly oscillatory zoned rims (Fig. 5). A total of 29 analyses were conducted on 29 grains with oscillatory zoning structure, yielding a large range of apparent $^{207}Pb/^{206}Pb$ ages of 2509–3568 Ma (Supplementary Table S1). Excluding the eight older and scattered analyses (2735–3568 Ma), the other 21 analyses showed a narrow range of apparent ages of 2509–2561 Ma. They yielded the upper intercept age of 2530±6 Ma (MSWD=0.82) and a weighted mean age of 2526±9 Ma (MSWD=0.41; Fig. 6c), of which the latter is taken as the best estimate of crystallization age of the granitic precursors.

Sample 14BB47-1 is a late Neoarchean coarse-grained potassium granite collected near Shitang Village, 20 km east of Fengyang County (32.82095° N, 117.73047° E; Fig. 2). It consists predominantly of quartz and K-feldspar (>90%) with minor plagioclase and biotite, with most plagioclase altered to sericite. Most zircon grains from this sample are elongated and prismatic with average crystal length of 100–150 μm and length/width ratios of 1.5:1–2:1 (Fig. 5). CL images showed oscillatory zoning cores indicative of magmatic growth, and most of them had a thin overgrowth or recrystallization rim (Fig. 5). A total of 27 analyses on the oscillatory-zoned cores gave apparent $^{207}Pb/^{206}Pb$ ages of 2506–2556 Ma (Supplementary Table S1), yielding an upper intercept age of 2536±14 Ma (MSWD=0.57) and a weighted mean age of 2524±8 Ma (MSWD=0.82) within analytical error (Fig. 6d), of which the latter is interpreted as the crystallization age of the potassium granite. A total of 22 analyses on the structureless rims with Th/U ratios of 0.02–1.31 have apparent $^{207}Pb/^{206}Pb$ ages of 2486–2524 Ma (Supplementary Table S1), yielding an upper intercept age of 2515±9 Ma (MSWD=0.27) and a weighted mean age of 2509±10 Ma (MSWD=0.19; Fig. 6d), indicating an end-Archean metamorphic event just after emplacement of the granitic magma.

Sample 14BB49-1 is a late Neoarchean monzogranite collected from a roadside outcrop near Mashan Village (32.93804° N, 117.76530° E; Fig. 2). It has a mineral assemblage similar to that of Sample 14BB47-1, with plagioclase (40%), K-felsdpar (25%), quartz (20%) and minor opaque minerals. Some zircon grains from this sample are elongated and prismatic, showing oscillatory zoned cores surrounded by thin overgrowth or recrystallization rims, whereas others are short and round, and have grey nebulous patterns (Fig. 5). A total of 35 analyses performed on oscillatory zoned cores yielded apparent $^{207}Pb/^{206}Pb$ ages of 2488–2561 Ma (Supplementary Table S1), giving an upper intercept age of 2533±10 Ma (MSWD=0.43) and a weighted mean age of 2525±9 Ma (MSWD=0.49; Fig. 6e). A total of 21 analyses of nebulous domains showed slightly younger apparent ages of 2477–2517 Ma (Supplementary Table S1), with an upper intercept age of 2495±9 Ma (MSWD=0.38) and a weighted mean age of 2490±12 Ma

https://doi.org/10.1017/S0016756818000869 Published online by Cambridge University Press

Table 1. Summary of the zircon U–Pb data of major lithologies from the Bengbu and Huoqiu areas at the southeastern NCC

Sample	Rock type	Geological units	Crystallization age (Ma)	Inherited or detrital zircon age (Ma)	Metamorphic age (Ma)	Method	References
Jiagou and Nushan xenoliths							
NS314	Intermediate granulite	Nushan basanites			1915±27	SHRIMP	Huang et al. (2004)
05JG-6	Garnet pyroxene amphbolite	Jiagou dioritic porphyrite			1904±53	SHRIMP	Guo & Li (2009)
07JG12	Meta-basic rock	Jiagou dioritic porphyrite			1800±15	SHRIMP	Liu *et al.* (2009)
07JG14	Meta-basic rock	Jiagou dioritic porphyrite			1811±19	SHRIMP	Liu *et al.* (2009)
07JG34	Mafic granulite	Jiagou dioritic porphyrite	2480±49	2602–2759	2167±58	SHRIMP	Liu *et al.* (2013*a*)
07JG32	Felsi garnt gneiss	Jiagou dioritic porphyrite	2121±32		1805±43	SHRIMP	Liu *et al.* (2013*a*)
08JG18	Mafic garnet-bering granulite	Jiagou dioritic porphyrite	2552±13	2635–2660	2473±15	SHRIMP	Wang *et al.* (2012*a*)
08JG34	Granitic gneiss	Jiagou dioritic porphyrite	2641±8		2486±8	SHRIMP	Wang *et al.* (2012*a*)
Bengbu area							
BB0	Garnet plagioclase pyroxenite				1833±8	LA-ICP-MS	Xu *et al.* (2006)
BB8	Potassim granite	Zhuangzili pluton	2100±14	2485		LA-ICP-MS	Yang *et al.* (2009)
04FY-3	Retrograded garnet amphibolite	Wuhe Group			1870±10	SHRIMP	Guo & Li (2009)
05SMS-1	Flesh pink granite	Shimenshan pluton	2058±8			SHRIMP	Guo & Li (2009)
07SMS	Potassim granite	Shimenshan pluton	2096±9			LA-ICP-MS	Wang *et al.* (2017*a*)
1403FY13-5	Granitic gneiss		2096±8		1848±7	LA-ICP-MS	Wang *et al.* (2017*a*)
14BB19-2	Plagioclase amphibolite	Wuhe Group	2126±37	2361–2683		LA-ICP-MS	Liu *et al.* (2018)
14BB08-2	Granite porphyry		2147±29	2340–2554	1844±17	LA-ICP-MS	this study
14BB37-1	Granite		2132±8			LA-ICP-MS	this study

(*Continued*)

Table 1. (*Continued*)

Sample	Rock type	Geological units	Crystallization age (Ma)	Inherited or detrital zircon age (Ma)	Metamorphic age (Ma)	Method	References
14BB40-1	Potassic granite		2183±16	2320–2696		LA-ICP-MS	this study
14BB41-1	Monzogranitic gneiss		2526±9	2735–2966		LA-ICP-MS	this study
14BB47-1	Potassium granite		2524±8		2509±10	LA-ICP-MS	this study
14BB49-1	Monzogranite		2525±9		2490±12	LA-ICP-MS	this study
14BB35-1	Granodioritic gneiss		2731±9	2802–2918	2524±41	LA-ICP-MS	this study
14BB44-1	Granodioritic gneiss		2929±7			LA-ICP-MS	this study
14BB07-3	Calcite quartzite	Wuhe Group			1846±15	LA-ICP-MS	Liu *et al.* (2018)
14BB29-3	Diopside marble	Wuhe Group			1819±7	LA-ICP-MS	Liu *et al.* (2018)
14BB29-4	Marble	Wuhe Group			1815±7	LA-ICP-MS	Liu *et al.* (2018)
14BB30-1	Dolomite-bearing marble	Wuhe Group			1855±10	LA-ICP-MS	Liu *et al.* (2018)
14BB31-3	Dolomite-bearing marble	Wuhe Group			1830±12	LA-ICP-MS	Liu *et al.* (2018)
07FY01	Garnet amphibolite				1839±31	SHRIMP	Liu *et al.* (2009)
07MJ4	Granulite	Wuhe Group			1876±18	SHRIMP	Wang *et al.* (2013)
Huoqiu area							
313ZX84-3	Magnetite amphibolite	Huoqiu Group	2711±31	2895–3065		LA-ICP-MS	Yang *et al.* (2012)
HQ0708	Gneissic tonalite	Huoqiu Group	2754±13		1842±17	SHRIMP	Wan *et al.* (2010)
HQ0704	Banded tonalite	Huoqiu Group	2564±25	2686–2690		SHRIMP	Wan *et al.* (2010)
FJZK01-171	Augen potassic granite	Huoqiu Group	2708±50			LA-ICP-MS	Wang *et al.* (2014*a*)
NZZK01-324	Migmatitic syenogranite	Huoqiu Group	2709±21			LA-ICP-MS	Wang *et al.* (2014*a*)
ZK122-2	Orthogneiss	Huoqiu Group	2711±25	2799–2929		LA-ICP-MS	Liu *et al.* (2015*a*)
ZK3-511	Orthogneiss	Huoqiu Group	2765±11			LA-ICP-MS	Liu *et al.* (2015*a*)
ZX34-40	Orthogneiss	Huoqiu Group	2752±24		2444±29	LA-ICP-MS	Liu *et al.* (2015*a*)

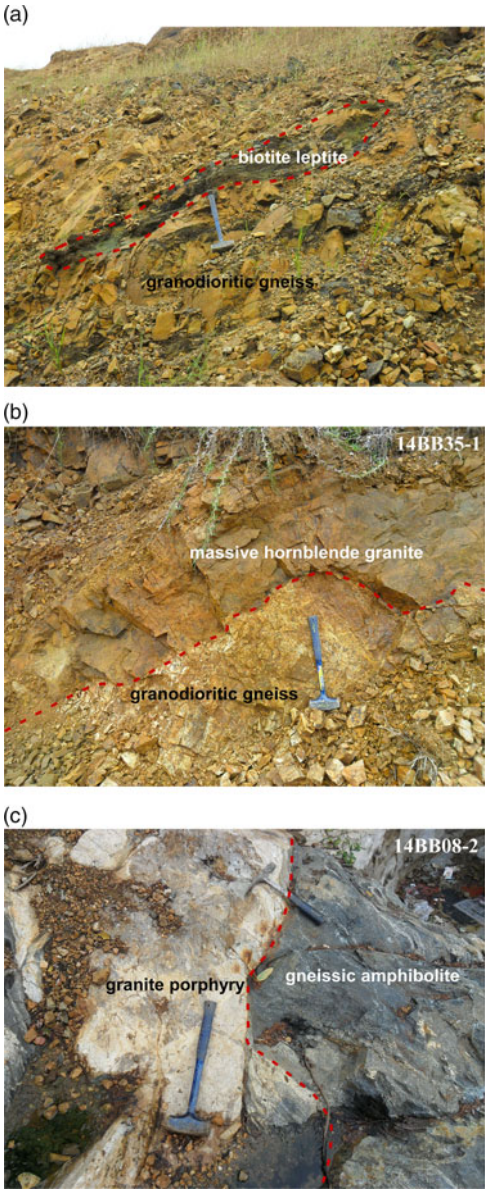

Fig. 3. (Colour online) Field photographs of Archean–Palaeoproterozoic (gneissic) granitoids in the Bengbu area: (a) dark biotite leptite occurs as enclaves in the Mesoarchean granodioritic gneiss sample (14BB44-1); (b) an early Neoarchean granodioritic gneiss sample (14BB35-1) is intruded by a Mesozoic dark hornblende granite; and (c) a middle Palaeoproterozoic biotite-bearing granite porphyry (14BB08-2) intrudes into dark gneissic amphibolites. The hammer is 30 cm in length.

(MSWD=0.16; Fig. 6e). On the basis of zircon internal structures, the monzogranite emplaced at 2525±9 Ma and was subjected to a later (2490±12 Ma) tectonothermal event.

Sample 14BB08-2 is a middle Palaeoproterozoic biotite-bearing granite porphyry collected *c.* 3 km SW of Huaiyuan County (32.93130° N, 117.22049° E; Fig. 2), where it intrudes into dark gneissic amphibolites (Fig. 3c). It is characterized by porphyritic texture with quartz (15%), plagioclase (25%), biotite (10%) and K-feldspar (5%) phenocrysts surrounded by groundmass of fine-grained plagioclase and quartz (Fig. 4d). Zircon grains separated from this sample show stubby or oval shapes, with lengths and length/width ratios of 70–100 μm and 1:1–1.5:1, respectively (Fig. 5). In the CL images, some grains show blurred oscillatory zoning cores corroded by bright homogeneous rims, whereas others display nebulous patterns (Fig. 5). A total of 16 analyses were conducted on the oscillatory zoning domains, which plot on or close to corcordia and show apparent $^{207}Pb/^{206}Pb$ ages ranging over 2124–2554 Ma with Th/U ratios of >0.2 (Supplementary Table S1). With the exception of six older analyses of 2340–2554 Ma, the majority of results yielded similar apparent ages of 2124–2177 Ma with an upper intercept age of 2155±26 Ma (MSWD=2.0) and a weighted mean age of 2147±29 Ma (MSWD=0.87; Fig. 6f). Considering the occurrence of magmatic zircons of age 2360 and 2569 Ma in the gneissic amphibolites intruded by this sample (Liu *et al.* 2018), the weighted mean age of 2147±29 Ma is taken as the best estimate of the crystallization age of the granite porphyry. On the other hand, 17 analyses on the structureless rims and nebulous domains yielded a narrow range of apparent ages of 1821–1872 Ma, defining the upper intercept age of 1856±17 Ma (MSWD=0.49) and the weighted mean age of 1844±17 Ma (MSWD=0.29; Fig. 6f), consistent with the 1.8–1.9 Ga high-pressure granulite-facies metamorphism reported in the Bengbu area (Xu *et al.* 2006; Guo & Li, 2009; Liu *et al.* 2009; Wang *et al.* 2013; Liu *et al.* 2017*c*, 2018).

Another middle Palaeoproterozoic granitic sample (14BB37-1) was collected near Xiaoxi Village (33.03242° N, 117.92723° E; Fig. 2) and *c.* 3 km north of the Zhuangzili pluton. The sample has a massive structure and a mineral assemblage of plagioclase (45%), quartz (45%), K-feldspar (5%) and accessory muscovite and zircon (Fig. 4e). Zircon grains separated from this rock show elongated to stubby shapes, with lengths and length/width ratios of 100–200 μm and 1:1–2:1, respectively (Fig. 5). CL images reveal complex core-rim structures, with oscillatory and blurred zoning cores surrounded by narrowly patchy or structureless rims (Fig. 5). A total of 56 analyses were conducted on 56 zircon cores, and the data plot near or on the concordia line (Fig. 6g). They show apparent $^{207}Pb/^{206}Pb$ ages of 2118–2166 Ma, yielding an upper intercept age of 2137±6 Ma (MSWD=0.39) and a weighted mean age of 2132±8 Ma (MSWD=0.27; Fig. 6g). In consideration of the oscillatory zoning structures, positive Ce anomalies, negative Eu anomalies, steep HREE patterns (Fig. 8d), and high Th/U ratios (Fig. 7d), the weighted mean age of 2132±8 Ma is considered to be the crystallization age of the rock.

A middle Palaeoproterozoic massive potassic granite (Sample 14BB40-1) was collected near Gupei Village, c. 3 km south of the Zhuangzili pluton (32.97668° N, 117.92862° E; Fig. 2). It consists of quartz (40%), K-feldspar (40%), muscovite (10%), feldspar (5%) and minor biotite ilmenite and amphibole (Fig. 4f). Most zircon grains from this sample showed elongated and prismatic shapes, with a minor population exhibiting stubby shapes (Fig. 5). Their lengths and length/width ratios ranged over 100–200 μm and 1:1–2.5:1, respectively (Fig. 5). Most were characterized by blurred to clearly oscillatory and banded zonings, whereas some had nebulous domains in the CL images (Fig. 5). A total of 41 analyses were conducted on 41 oscillatory and banded zoning domains, and the data plot on or close to the concordia (Fig. 6h). These analyses yield apparent $^{207}Pb/^{206}Pb$ ages of 2172–3524 Ma with generally high Th/U ratios of 0.23–1.66 (Supplementary Table S1). On the probability density diagram, these analyses can be divided into three age groups. The oldest group is composed of 13 analyses and has the apparent age range 2736–2786 Ma, yielding the intercept age of 2766±9 Ma (MSWD=1.2) and the weighted mean age of 2757±14 Ma (MSWD=1.3; Fig. 6h). The middle group is composed of 14 analyses with apparent ages of 2506–2559 Ma, yielding the weighted mean age of 2530±13 Ma (MSWD=1.5; Fig. 6h). The youngest age group consists of five analyses and has an apparent age range of 2172–2177 Ma, yielding

https://doi.org/10.1017/S0016756818000869 Published online by Cambridge University Press

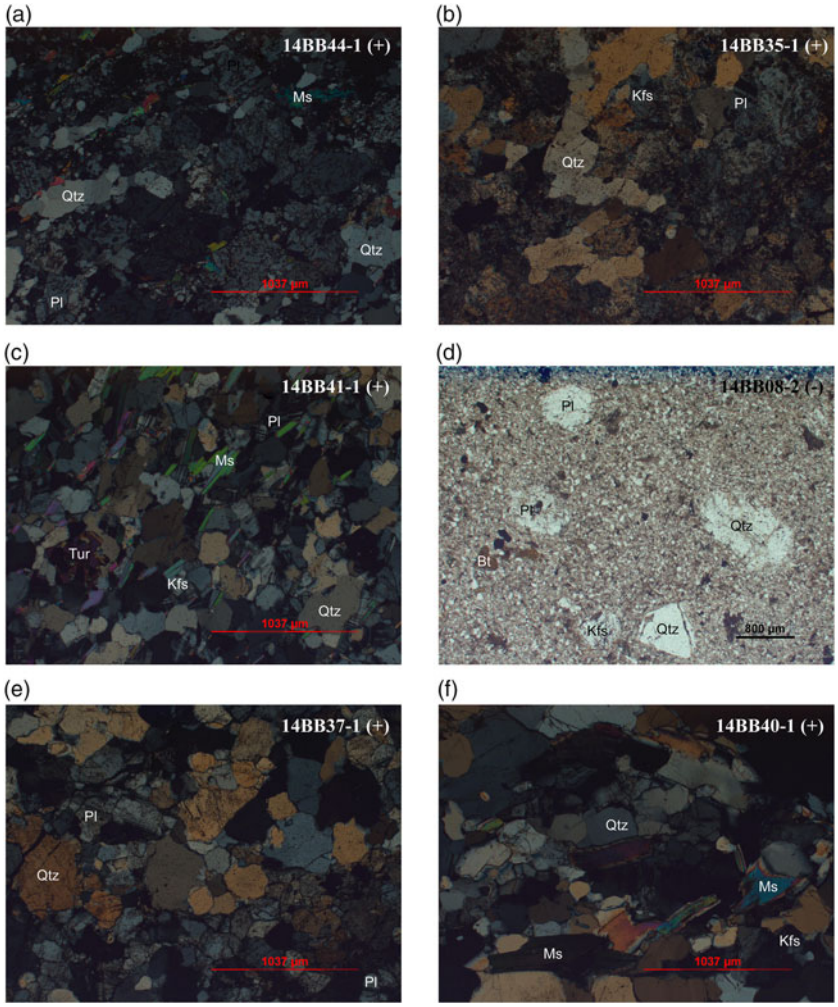

Fig. 4. (Colour online) Microscopic features of representative Archean–Palaeoproterozoic (gneissic) granitoids in the Bengbu area. (+): viewed under crossed polarized light; (–): viewed under plane polarized light. Abbreviations: Pl – plagioclase; Kfs – potassic feldspar; Qzt – quartz; Ms – muscovite; Tur – tourmaline.

the upper intercept age of 2183±16 Ma (MSWD=0.14; Fig. 6h). Considering the wide occurrence of magmatic zircons of age 2.53 and 2.75 Ga in the study region (Wan *et al.* 2010; Yang *et al.* 2012; Wang *et al.* 2012*a*, 2014*a*; Liu *et al.* 2015*a*; this study) and the absence of signs of a later tectonothermal event, the youngest upper intercept age of 2183±16 Ma is taken as the best estimate of the intruding age.

4.b. Zircon trace-element composition

To investigate the possible involvement of hydrothermal zircons, we used a Ce/Ce^{*} ratio of 3.5 and $(Sm/La)_N$ ratio of 4.4 (Hoskin, 2005) as thresholds, allowing the zircons with lower ratios to be discarded. The entire dataset describing the magmatic zircon trace-element composition, selected ratios and statistical descriptions of the distributions classified by different ages is provided in online Supplementary Table S2 (available at http://journals.cambridge.org/geo), and the representative ratios and chondrite-normalized REE patterns are plotted in Figures 7 and 8, respectively. The means are calculated after removing outliers, and standard deviations relative to the means for each age group are reported. In addition, Figure 9 clearly shows that there are no apparent correlations between zircon Th/U, U/Yb and Yb/Gd ratios with Ti contents, indicating that the fractional crystallization process does not affect these ratios significantly. Nearly constant Th/U ratios for every zircon population may be explained by slightly changed fractionation factor $(Th_{(zircon/rock)}/U_{(zircon/rock)})$ below 800 °C (Kirkland *et al.* 2015). On the other hand, the narrow range of U/Yb and Yb/Gd ratios are probably due to absence of minerals (such as garnet and hornblende) in the HREEs in the fractional crystallization process. The average values and ratios can therefore generally indicate their source reservoirs.

Ti concentrations divide the late Mesoarchean – middle Palaeoproterozoic zircons into two overlapping but distinct populations (Fig. 7a). The population aged 2.13–2.17 Ga (8.08±3.38 ppm) is shifted towards higher Ti concentrations than the populations aged 2.53 (5.10±2.58 ppm), 2.73 (4.53±1.29 ppm) and 2.93 Ga (6.52±3.78 ppm). If we assume a_{TiO2} and a_{SiO2} of unity, the estimates represent minimum temperatures (Ferry & Watson, 2007). The mean calculated middle Palaeoproterozoic zircon growth temperature is 718±44 °C, much higher than that for the late Neoarchean (677±46 °C), the early Neoarchean zircons (674±22 °C) and the late Mesoarchean (699±41 °C), calculated using the same activities.

Chondrite-normalized REE patterns for all the magmatic zircons in this study are generally typical of those reported from igneous rocks (Fig. 8): HREEs are extremely enriched relative to LREEs, and positive Ce and negative Eu anomalies are ubiquitous. However,

https://doi.org/10.1017/S0016756818000869 Published online by Cambridge University Press

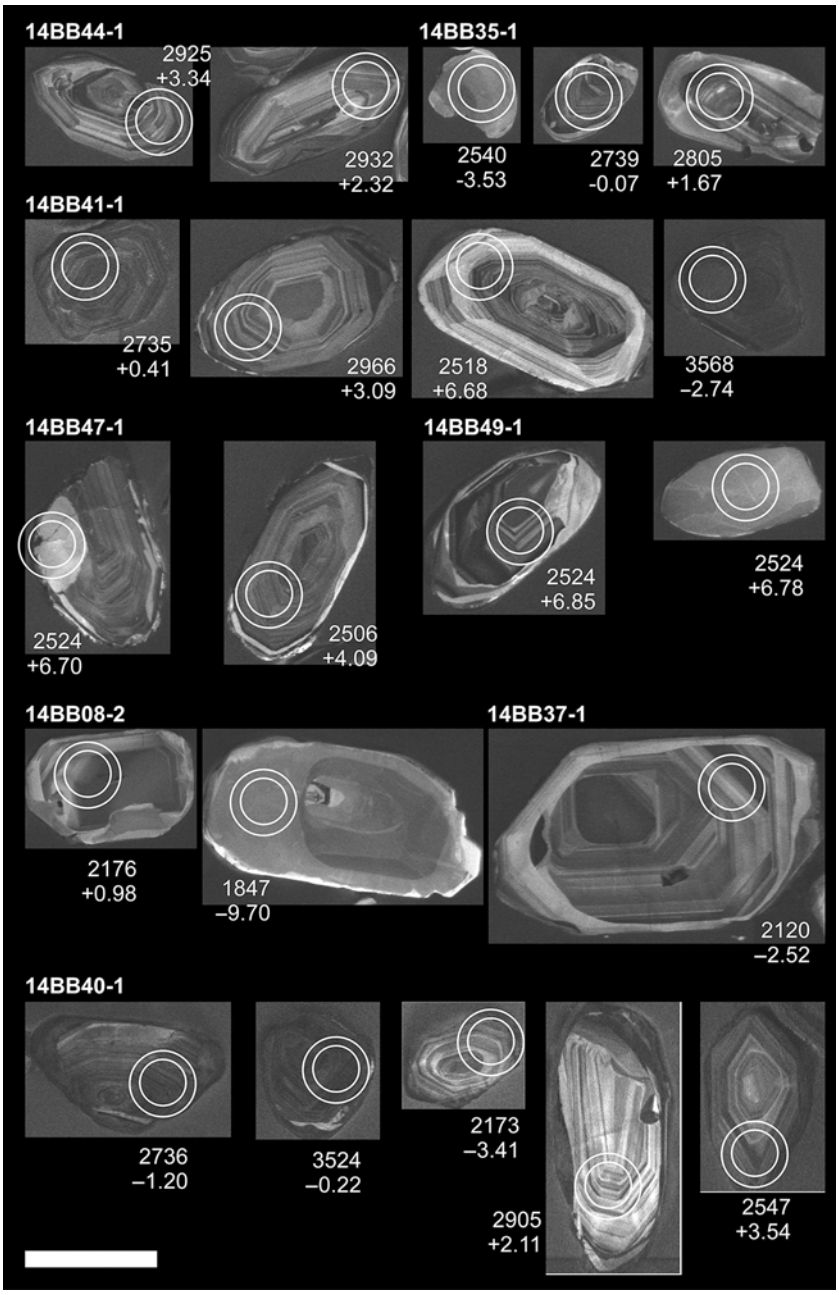

Fig. 5. Representative selection of cathodoluminescence (CL) zircon images. Circles (50 and 35 μm) show positions of Lu–Hf and U–Pb analytical sites. $^{207}Pb/^{206}Pb$ ages and $\varepsilon_{Hf}(t)$ values are also plotted. The scale bar is 100 μm long.

HREE concentrations are much higher in the zircons aged 2.93 Ga, in which Yb concentrations have a median of 346±116 ppm. For the other three populations, Yb concentrations are much lower (209±75, 145±53 and 182±90 ppm for the zircons aged 2.13–2.17 Ga, 2.53 Ga and 2.73 Ga, respectively). On the other hand, the Yb/Gd ratios, which are thought to correlate changes in crustal thickness (Barth *et al.* 2013), divide the zircons into two groups: mean ratio of the zircons aged 2.13–2.17 Ga is 15.1±4.0 ppm, whereas the mean ratios of the zircons aged 2.53, 2.73 and 2.93 Ga are 11.3±4.2, 12.5±2.2 and 11.5±2.0 ppm, respectively (Fig. 7b).

Trace elements in igneous zircon can be used both as general means to relate their formation to a general tectonic setting and as more specific proxies for change in magma compositions (Hoskin, 2005; Carley *et al.* 2014; Grimes *et al.* 2015). For example, the U/Yb ratio has been used as a proxy for subducting slab fluid addition because the fluids are enriched in U relative to HREEs such as Yb (Barth *et al.* 2013). Our zircons yield U/Yb ratios which increase from those aged 2.93 Ga (0.34±0.12) to 2.73 Ga (0.96±0.42) and to 2.53 Ga (1.05±0.46), but there is an evident decrease at age 2.13–2.17 Ga (0.61±0.40; Fig. 7c). On the other hand, the Th/U ratios have been successfully employed as a proxy for crustal input based on the enrichment in Th over U as the crust matures (Barth *et al.* 2013). Two obvious changes can be observed in our data set: a decrease in Th/U ratios from 2.93 Ga (0.63±0.12) to 2.73 Ga (0.27±0.09) and an increase from 2.73 Ga to 2.53 Ga (0.62±0.22; Fig. 7d).

https://doi.org/10.1017/S0016756818000869 Published online by Cambridge University Press

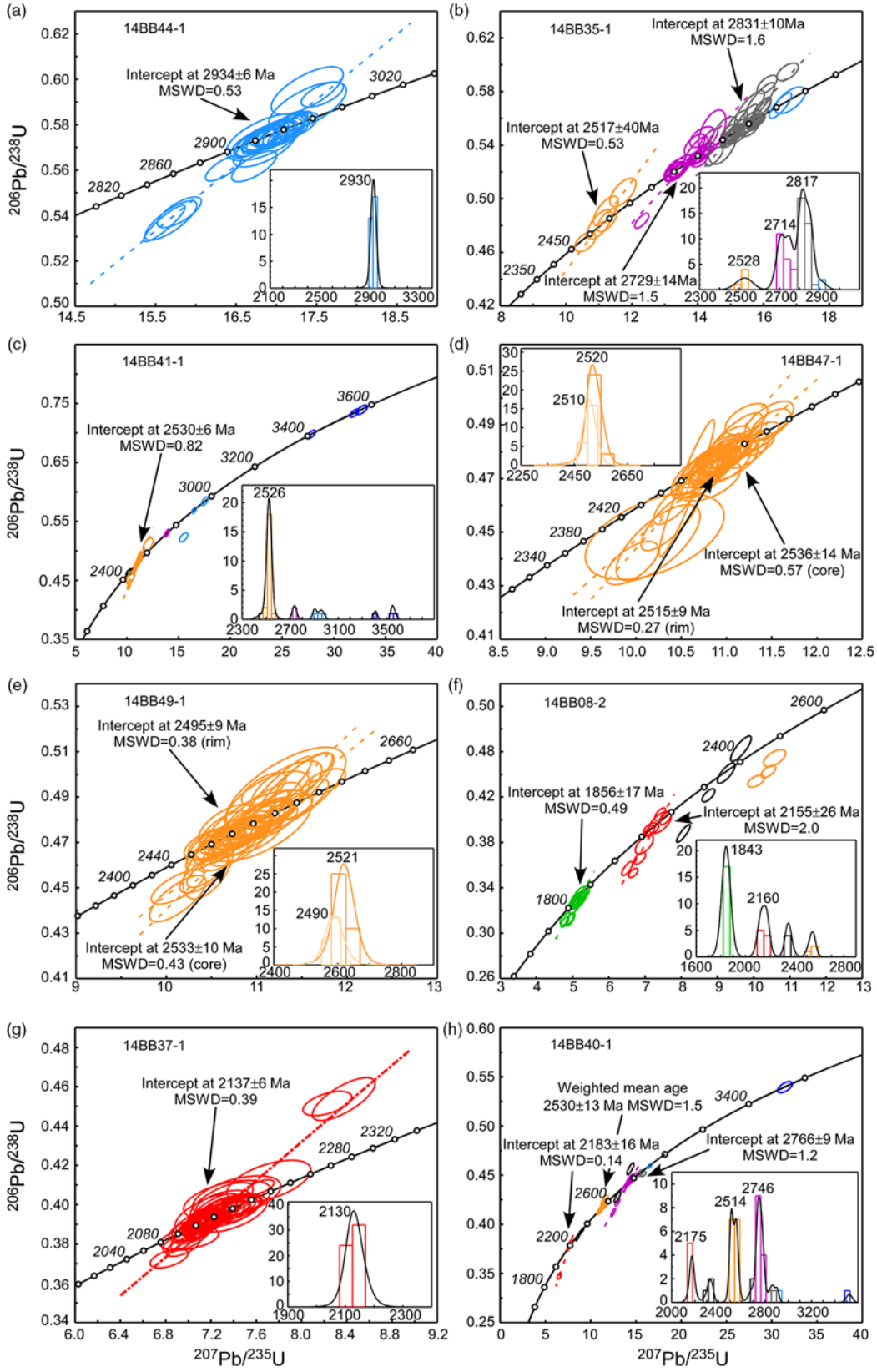

Fig. 6. (Colour online) Concordia diagrams for all the nearly concordant or concordant zircon spots from the (gneissic) granitoids in the Bengbu area, showing histogram of the apparent $^{207}Pb/^{206}Pb$ ages (insets).

https://doi.org/10.1017/S0016756818000869 Published online by Cambridge University Press

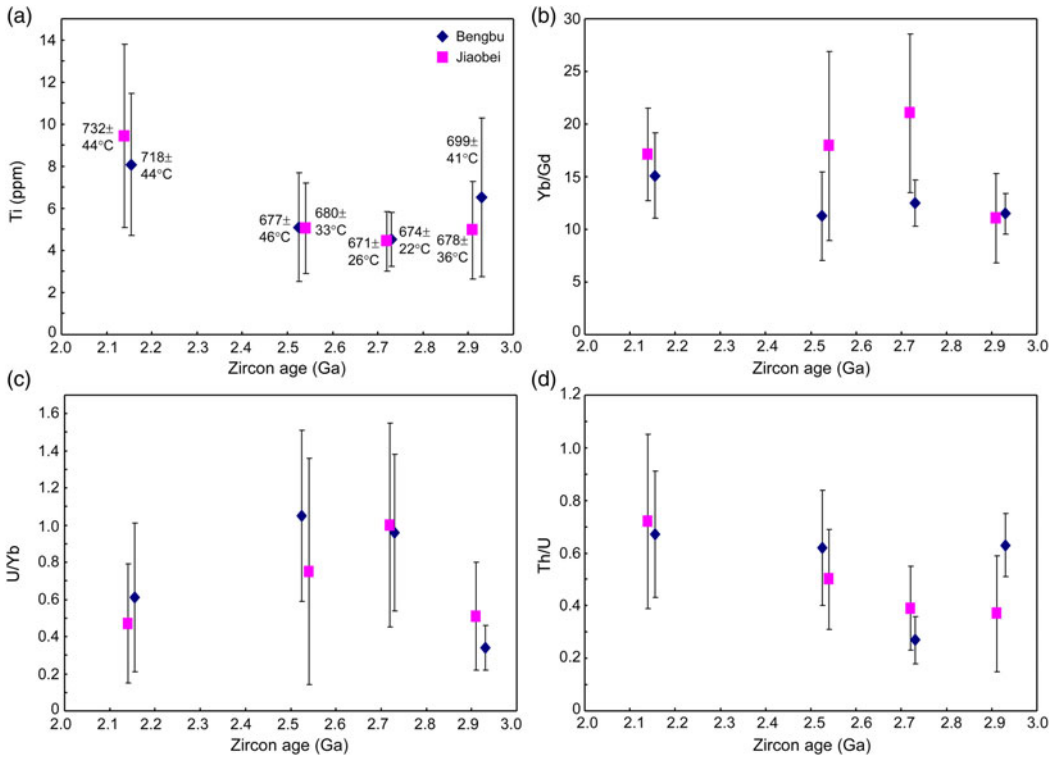

Fig. 7. (Colour online) Comparisons of zircon trace-element and representative ratios of the Bengbu and Jiaobei granitoids. The average values and the standard deviations are plotted. *X*-axis represent crystallization age of the granitoids.

4.c. Zircon Lu–Hf isotopes

Magmatic and metamorphic zircons with concordant ages from the five granitic samples and three granitic gneiss samples from the Bengbu area were analysed for Lu–Hf isotopes, and the results are listed in online Supplementary Table S3 (available at http://journals.cambridge.org/geo) and plotted in Figure 10 in the $\varepsilon_{Hf}(t)$ versus $^{207}Pb/^{206}Pb$ age plots.

Calculated at the apparent $^{207}Pb/^{206}Pb$ age (t_1), most analyses of the youngest group of magmatic zircons for each sample yield nearly consistent $^{176}Hf/^{177}Hf(t_1)$ ratios: 0.280955–0.281045 for 14BB44-1, 0.281030–0.281074 for 14BB35-1, 0.281289–0.281341 for 14BB47-1, 0.281329–0.281383 for 14BB49-1, 0.281425–0.281453 for 14BB08-2, 0.281362–0.281444 for 14BB37-1 and 0.281303–0.281379 for 14BB40-1 (Supplementary Table S3). This implies that, with the exception of the magmatic zircons of 14BB41-1 aged *c.* 2.53 Ga, which yield a large range of $^{176}Hf/^{177}Hf(t_1)$ ratios of 0.281034–0.281364 (Supplementary Table S3), the youngest group of magmatic zircons of the other seven samples crystallized from the same magmatic system and was subjected to limited degrees of subsequent Pb loss (Zeh *et al.* 2010). On the other hand, the large range of $^{176}Hf/^{177}Hf(t_1)$ ratios for the magmatic zircons of the monzogranitic gneiss 14BB41-1 aged *c.* 2.53 Ga, in combination with the presence of muscovite and tourmaline (Fig. 4c) and the Palaeoarchean – early Neoarchean xenocrystic zircons (Fig. 6c), may reflect different degrees of mixing of crustal sources.

Magmatic zircon U–Pb ages in this study can be generally divided into five populations according to age: 3.41–3.57 Ga, 2.91–2.95 Ga, 2.70–2.76 Ga, 2.49–2.56 Ga and 2.05–2.19 Ga. All the Palaeoarchean xenocrystic zircons were found from the potassium granites (Samples 14BB40-1 and 14BB41-1) on the eastern margin of the study area, and the analysed four grains have negative $\varepsilon_{Hf}(t)$ values of −3.81 to −0.22 and T_{DM2} model ages of 3.80–3.99 Ga (Fig. 10c and h), suggesting their origin from an Eoarchean crust. For the late Mesoarchean zircon population, most of their $\varepsilon_{Hf}(t)$ values are positive and more than two units lower than the value of the temporal depleted mantle (DM; +1.25 to +5.29; Fig. 10a, c, h) and have T_{DM2} model ages of 3.02–3.24 Ga, indicative of the recycling of an early Mesoarchean crust. The early Neoarchean zircons have a narrow range of $\varepsilon_{Hf}(t)$ values near to zero (−1.73 to +1.89) and T_{DM2} model ages of 3.07–3.29 Ga (Fig. 10b, c, h), similar to those of the late Mesoarchean zircons. Magmatic zircons with ages of 2.49–2.56 Ga from 14BB47-1 and 14BB49-1 have narrow ranges of $\varepsilon_{Hf}(t)$ values and T_{DM2} model ages of +3.83 to +7.52 and 2.56–2.77 Ga, respectively (Fig. 10c, d, e, h), indicating a significant juvenile crustal growth event with limited recycling of early Neoarchean crust. On the other hand, the large range of $\varepsilon_{Hf}(t)$ values and T_{DM2} model ages of −4.90 to +6.68 and 2.60–3.99 Ga, respectively, from 14BB40-1 and 14BB41-1 suggest different degrees of mixing of Eoarchean – early Neoarchean crust with juvenile addition. The zircons with ages of 2.12–2.18 Ga have a very large range of $\varepsilon_{Hf}(t)$ values of −7.49 to +0.98 and T_{DM2} model ages of 2.65–3.20 Ga (Fig. 10f, g, h), indicating recycling of the Mesoarchean–Neoarchean crust.

On the other hand, the end-Archean metamorphic zircons from samples 14BB47-1 and 14BB49-1 have $\varepsilon_{Hf}(t)$ values and T_{DM2} model ages of +7.33 to +4.10 and 2.54–2.75 Ga, respectively (Fig. 10d, e), overlapping with those of the magmatic zircons from the same samples and indicating solid-state recrystallization (Hoskin & Black, 2000). The metamorphic zircon rims from Sample 14BB08-2 of age *c.* 1.84 Ga have strongly negative $\varepsilon_{Hf}(t)$ values of −11.35 to −3.40 and T_{DM} model ages of 2.69–3.19 Ga (Fig. 9f). In addition, all the metamorphic zircon rims of age *c.* 1.84 Ga have nearly identical $^{176}Hf/^{177}Hf$ ratios to those of the

https://doi.org/10.1017/S0016756818000869 Published online by Cambridge University Press

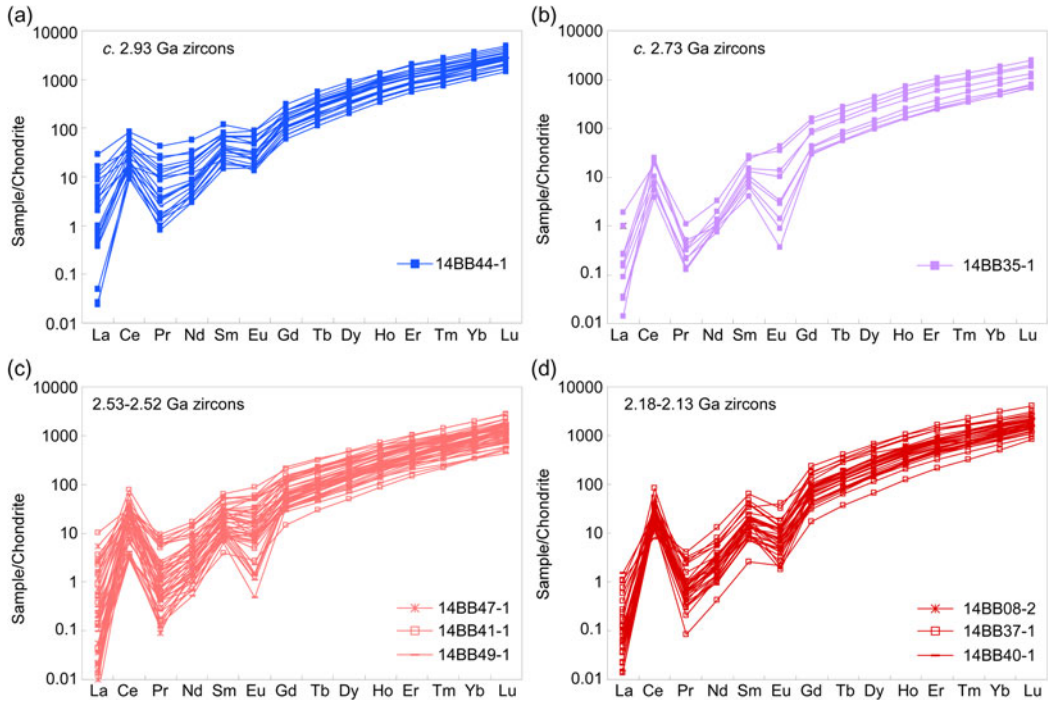

Fig. 8. (Colour online) Chondrite-normalized REE patterns for the youngest magmatic zircons from the Bengbu granitoids. Normalizing values after Sun & McDonough (1989).

magmatic cores aged *c.* 2.15 Ga, suggesting solid-state recrystallization similar to the end-Archean metamorphic zircons (Hoskin & Black, 2000).

5. Discussion

Zircon U–Pb geochronology and Lu–Hf isotopes obtained in this study and previous data of major lithologies from the Bengbu and Huoqiu areas are summarized in Table 1 and Figure 11, and are compared with zircon U–Pb, trace element and Lu–Hf data from the Jiaobei Terrane.

5.a. Geochronological framework of the Bengbu and Huoqiu areas

Magmatic zircons of a granodioritic gneiss (14BB44-1) from the southeastern Bengbu area have a Mesoarchean age of 2929±7 Ma, which is consistent with the 2.97 Ga zircons from an amphibolite collected from drill cores in the Huoqiu area (Liu *et al.* 2015*a*). These magmatic zircon ages suggest the existence of late Mesoarchean crust in the southeastern NCC, which is further supported by the xenocrystic zircons aged 2.90–2.95 Ga from a magnetite amphibolite (Yang *et al.* 2012) and TTG gneisses (Liu *et al.* 2015*a*) in the Huoqiu area, and xenocrystic zircons aged 2.90–2.97 Ga from a granodioritic gneiss (14BB35-1) and a monzogranitic gneiss (14BB41-1) in the Bengbu area (this study). In addition, the early Neoarchean magmatic zircon age of 2731±9 Ma has been obtained from a granodioritic gneiss (14BB35-1), which matches the zircon ages of 2.71–2.76 Ga from the TTG gneisses, migmatic syenogranite, potassic granite and plagioclase amphibolite (Wan *et al.* 2010; Yang *et al.* 2012; Wang *et al.* 2014*a*; Liu *et al.* 2015*a*) in the Huoqiu area. On the other hand, a monzogranitic gneiss (14BB41-1), a potassium granite (14BB47-1) and a monzogranite (14BB49-1) give end-Neoarchean zircon ages of 2526±9, 2524±8 and 2525±9 Ma, respectively, which are in good agreement with previously published zircon U–Pb ages of 2.56 Ga from a gneissic tonalite in the Huoqiu area (Wan *et al.* 2010) and an age of 2.55 Ga from a garnet-bearing basic gneiss xenolith from the Jiagou Mesozoic intrusion (Wang *et al.* 2012*a*). The last major early Precambrian episode of magmatism occurred during the middle Palaeoproterozoic Era, as evidenced by the 2147±29 Ma granite porphyry (14BB08-2), the 2132±8 Ma granite (14BB37-1) and the 2183±16 Ma potassic granite (14BB40-1), which are slightly older than the 2.06–2.10 Ga Shimenshan and Zhuangzili plutons (Yang *et al.* 2009; Guo & Li, 2009; Wang *et al.* 2017*a*) and nearly the same with the 2.13 Ga plagioclase amphibolite of the Wuhe Group (Liu *et al.* 2018) and the 2121 Ma felsic garnet-bearing gneiss xenolith in the Jiagou intrusion (Liu *et al.* 2013*a*). In summary, all these geochronological data from the basement rocks and xenoliths in the Bengbu and Huoqiu areas suggest multistage magmatic events during the late Mesoarchean – middle Palaeoproterozoic period, with felsic magmatism occurring at *c.* 2.93, 2.76–2.71, 2.56–2.52 and 2.18–2.10 Ga, whereas mafic magmatism only occurred at 2.71, 2.55 and 2.13 Ga (Table 1 and Fig. 11a).

We also obtained metamorphic zircon ages of 2.49–2.52 Ga and 1.84 Ga from the major granitoid lithologies in the Bengbu area. Similar metamorphic zircon ages of 2.48–2.52 Ga have been previously reported from the Neoarchean – middle Palaeoproterozoic granitic gneisses (Wang *et al.* 2012*a*; Liu *et al.* 2015*a*) and basic granulite (Wang *et al.* 2012*a*). The metamorphic ages of *c.* 2.5 Ga are consistent with those reported from other Archean basement complexes in the Eastern Block of the NCC (e.g. Zhao *et al.* 1998; Ge *et al.* 2003; Geng *et al.* 2006; Yang *et al.* 2008; Liu *et al.* 2011; Lv *et al.* 2012; Wan *et al.* 2012; Wang *et al.* 2012*b*, 2015, 2017*b*; Wu *et al.* 2013), representing a large-scale end-Neoarchean tectonothermal event related to underplating of large amounts of mantle-derived magma in the Eastern Block (Zhao *et al.* 1998; Yang *et al.* 2008; Wu *et al.* 2013; Wang *et al.* 2015). On the other hand, similar late Palaeoproterozoic metamorphic ages have been found in nearly all the major basement lithologies in the study area (Xu *et al.* 2006; Guo & Li, 2009; Liu *et al.* 2009, 2017*c*, 2018; Wan *et al.* 2010;

https://doi.org/10.1017/S0016756818000869 Published online by Cambridge University Press

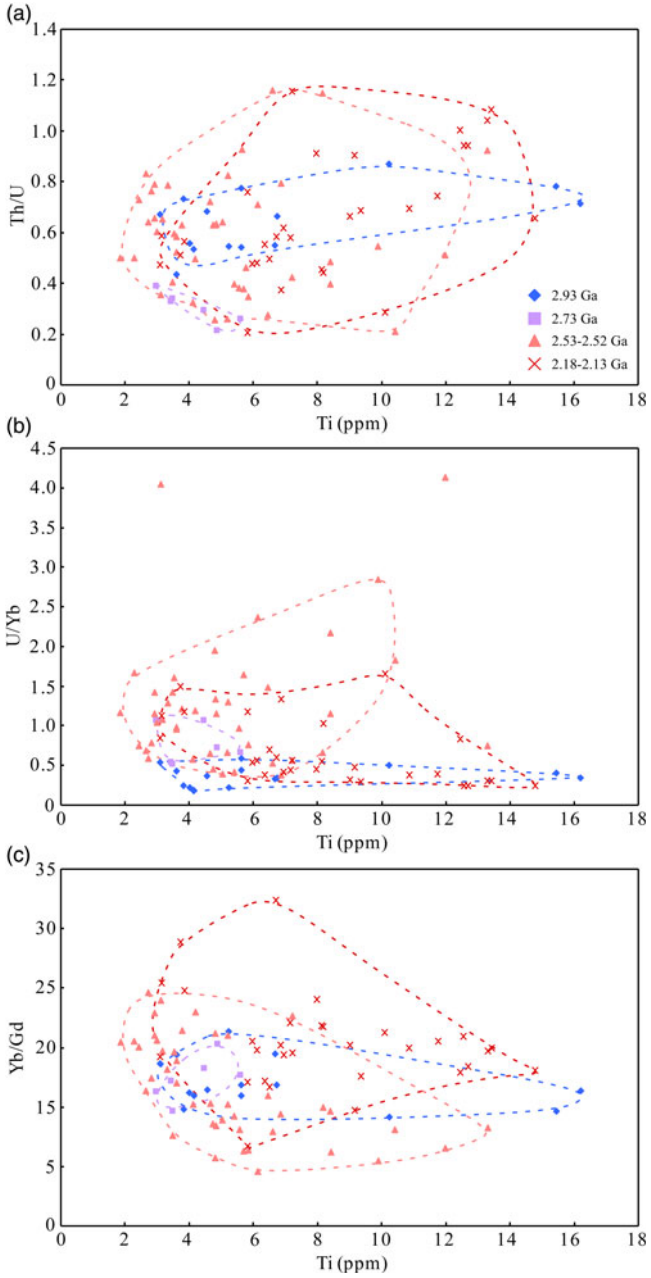

Fig. 9. (Colour online) Zircon (a) Th/U, (b) U/Yb and (c) Yb/Gd (c) ratios v. Ti (ppm) for the youngest magmatic zircons from the Bengbu granitoids.

Wang *et al.* 2017*a*) and xenoliths in the Jiagou intrusions (Guo & Li, 2009; Liu *et al.* 2009, 2013*c*), which are in good agreement with the timing of metamorphism of 1.96–1.80 Ga reported from other areas of the JLJB (Wan *et al.* 2006; Tang *et al.* 2007; Zhou *et al.* 2008*b*; Tam *et al.* 2011; Liu *et al.* 2012*a*, 2017*d*). In conclusion, all metamorphic zircon data suggest that the Bengbu and Huoqiu areas experienced regional metamorphism at *c.* 2.5 Ga and subsequently encountered reworking by a tectonothermal event that was related with the formation of the Palaeoproterozoic JLJB.

5.b. A Palaeoarchean – early Neoarchean micro-continent in the southeastern NCC

Numerous investigations have been performed on the formation and evolution of the early Precambrian metamorphic crystalline basement of the NCC, and the division of the NCC into the Eastern Block, the Western Block and the intervening Trans-North China Orogen has been generally accepted (Fig. 1; Guo *et al.* 2002; Zhao *et al.* 2005, 2012; Zhang *et al.* 2009; Liu *et al.* 2012*b*). However, the spatial distribution of pre-Archean continental domains in the craton is still difficult to determine because of the poor preservation of ancient rocks as a result of the early hotter crust and mantle upwellings of the Earth (Bell *et al.* 2014; Kamber, 2015) and long-acting erosive and tectonic processes similar to recent Earth history. Because of resistance to recrystallization during hydrothermal alteration, zircon U–Pb–Lu–Hf isotopic systems are one of the most useful tools for gaining detailed information about the formation, recycling and evolution of the early continental crust (Amelin *et al.* 1999, 2000; Kinny & Maas, 2003; Griffin *et al.* 2004; Hawkesworth & Kemp, 2006; Wu *et al.* 2007, 2008; Yang *et al.* 2008; Gerdes & Zeh, 2009; Harrison, 2009; Zeh *et al.* 2010; Diwu *et al.* 2013; Kenny *et al.* 2016).

Based on the spatial distribution of ancient (older than 2.6 Ga) rocks and detrital and xenocrystic zircons from Palaeoproterozoic or older rocks, Wan et al. (2015) have delineated three ancient terranes in the NCC: the Eastern, Southern and Central ancient terranes (Fig. 1). The Southern ancient terrane is located along the southern margin of the NCC and includes the Zhongtiao, Lushan, Dengfeng, Xinyang, Huoqiu and Bengbu areas from west to east. On the other hand, the Jiaobei Terrane was suggested to be in tectonic affinity with the Anshan-Benxi, eastern Hebei and western Shandong, all of which formed the Eastern ancient terrane (Fig. 1). However, the Jiaobei Terrane has a close spatial relationship with the Bengbu area if the *c.* 400 km sinistral strike-slip fault along the Mesozoic NE-striking Tan-Lu Fault is recovered (Zhao *et al.* 2016; Fig. 1). The obvious similarities between the zircon U–Th–Pb–Lu–Hf isotopic and trace-element features of the Jiaobei Terrane and the Bengbu and Huoqiu areas suggest that they constitute a Palaeoarchean–Neoarchean micro-continent in the southeastern NCC.

5.b.1. Palaeoarchean

Our zircon U–Th–Pb isotopic dating results reveal xenocrystic zircons of age 3.41–3.57 Ga from the late Neoarchean and middle Palaeoproterozoic potassium granites on the eastern margin of the Bengbu area. Other recent studies have also reported detrital zircons of age 3.23–3.66 Ga from the middle Palaeoproterozoic Fengyang and Wuhe groups (Liu & Cai, 2017; Liu *et al.* 2018). All the xenocrystic and detrital have negative $\varepsilon_{Hf}(t)$ values of −6.3 to −0.2 and T_{DM2} model ages of 3.8–4.1 Ga (Fig. 11b), indicating recycling of an Eoarchean crust. In the Jiaobei Terrane, detrital zircons of a similar age (3.34–3.68 Ga; Ji 1993; Liu *et al.* 2013*d*; Xie *et al.* 2014*b*) and xenocrystic zircon (3.45 Ga; Wang *et al.* 1998) have also been found, and their Lu–Hf isotopes show features consistent with those in the Bengbu area (Fig. 11b; Liu *et al.* 2013*d*).

On the other hand, a Palaeoarchean Beitai-Waitoushan microblock was delineated in the NE NCC by integrating the newly discovered migmatized gneisses and inherited zircons of age *c.* 3.45 Ga from the Neoarchean granitoids (Liu *et al.* 2017*a*). Unlike the Palaeoarchean zircons in the southeastern NCC, these zircons exhibit complicated source material, with most of their $\varepsilon_{Hf}(t)$ values plotted between the DM and CHUR (chondrite uniform reservoir) lines as opposed to below the CHUR line, implying a Palaeoarchean crustal growth event (Dong *et al.* 2017; Liu *et al.* 2017*a*). Similar zircon U–Pb ages and evidently different Lu–Hf

https://doi.org/10.1017/S0016756818000869 Published online by Cambridge University Press

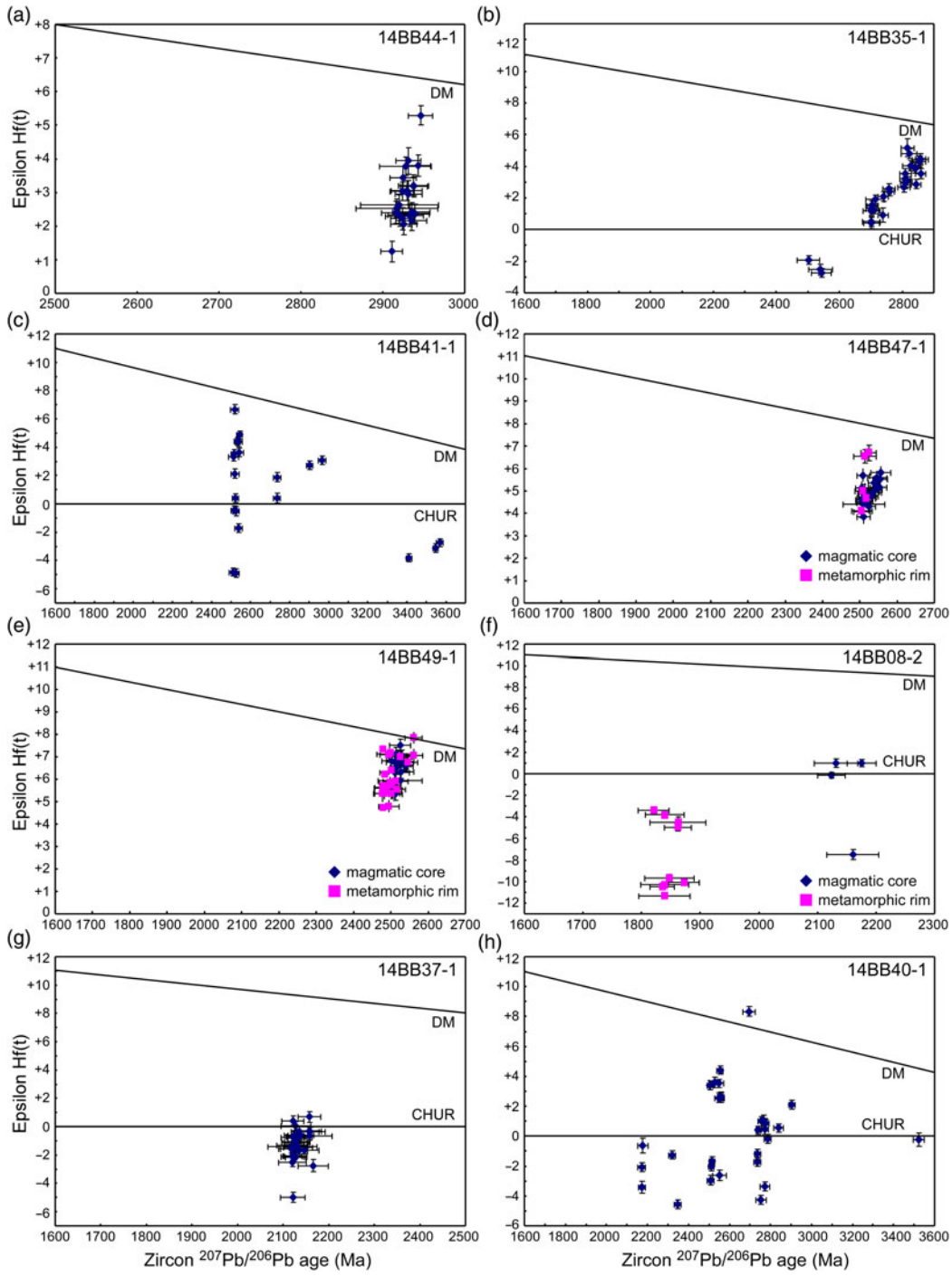

Fig. 10. (Colour online) Plots of $\varepsilon_{Hf}(t)$ vs. zircon age for each sample from the Bengbu area. CHUR – chondrite uniform reservoir; DM – depleted mantle.

isotopes are suggestive of at least two separated Palaeoarchean micro-blocks in the southeastern and northeastern NCC.

5.b.2. Late Mesoarchean

In the southeastern NCC, the TTG gneisses with magmatic zircon ages of 2.86–2.91 Ga were not only identified in the Jiaobei Terrane (Jahn *et al.* 2008; Liu *et al.* 2013*b*; Wu *et al.* 2014*a*; Wang *et al.* 2014*b*; Xie *et al.* 2014*a*), but also in the southeastern Bengbu area (2.93 Ga granodioritic gneiss; this study). Additionally, both whole-rock Nd and zircon Lu–Hf reveal that the protoliths of the late Mesoarchean TTG gneisses were derived mainly from juvenile sources (Fig. 11b; Jahn *et al.* 2008; Wu *et al.* 2014*a*, *b*; Xie *et al.* 2014*a*; this study). They are dominated by low-HREE-type TTG, indicative of a possible origin through partial melting of meta-basaltic rocks within a garnet-dominated stability field, under relative higher pressure at deeper depths (over 50 km; Wu *et al.* 2014*b*). Different tectonic settings have been proposed for these TTG gneisses, from partial melting of a subducted oceanic slab based on the Nb–Ti–P depletions (Jahn *et al.* 2008) to underplating of large amounts of mantle-derived magmas in consideration of the high SiO_2, low MgO, Cr and Ni contents (Xie *et al.* 2014*a*; Wu *et al.* 2014*b*).

https://doi.org/10.1017/S0016756818000869 Published online by Cambridge University Press

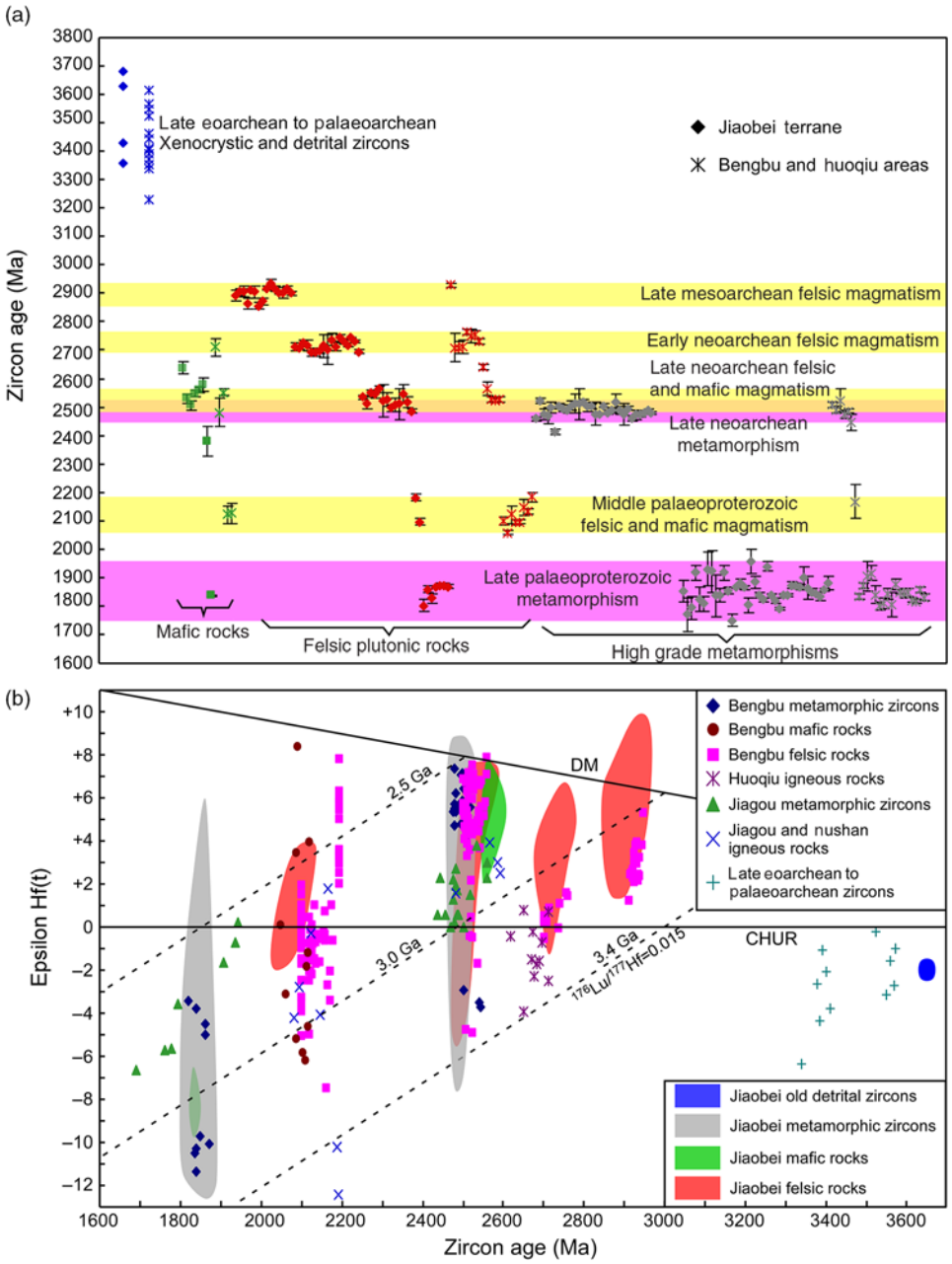

Fig. 11. (Colour online) (a) Summary of geochronology for late Eoarchean to late Palaeoproterozoic crustal evolution at the southeastern NCC, based on age data from Table 1. (b) Plots of $\varepsilon_{Hf}(t)$ v. zircon age for the major lithologies at the southeastern NCC. CHUR – chondrite uniform reservoir. DM – depleted mantle. Data source: Bengbu metamorphic zircon from Liu *et al.* (2018) and this study; Bengbu mafic rocks from Liu *et al.* (2018); Bengbu felsic rocks from Yang *et al.* (2009), Wang *et al.* (2017*a*) and this study; Huoqiu igneous rocks from Wang *et al.* (2014*a*) and Liu *et al.* (2015*a*); Jiagou metamorphic zircons from Liu *et al.* (2009, 2013*a*); Jiagou and Nushan igneous rocks from Wang *et al.* (2012*a*) and Liu *et al.* (2013*a*); late Eoarchean to Palaeoarchean zircon from Liu & Cai (2017), Liu *et al.* (2018) and this study; Jiaobei metamorphic zircons from Liu *et al.* (2013*b*), Wang *et al.* (2014*a*), Wu *et al.* (2014*a*), Zhang et al. (2014) and Xie *et al.* (2014*a*); Jiaobei mafic rocks from Wang *et al.* (2014*a*) and Wu *et al.* (2014*a*); Jiaobei felsic rocks from Liu *et al.* (2013*b*, 2014), Wu *et al.* (2014*a*), Xie *et al.* (2014*a*), Zhang et al. (2014), Shan et al. (2015) and Liu *et al.* (2017*d*).

The geochemistry of zircon provides an indication of its parental magma composition, and an integrated analysis of U–Pb age and Lu–Hf isotope and trace elemental concentration on a single crystal offers a powerful approach to constraining the source nature recorded by detrital or xenocrystic grains (Barth *et al.* 2013; Carley *et al.* 2014; Paulsen *et al.* 2016) and the rare Mesoarchean crust in the NCC due to a lack of other geological evidence. By compiling a global database of zircon trace-element composition from different tectonic settings, Carley *et al.* (2014) found that zircons from settings without subduction influence (mid-ocean-ridge basalt or MORB and evolving continental-oceanic rift settings) are distinct in composition from those from Phanerozoic arcs and even more so from Hadean zircons (Fig. 12a–c). The former group is most notably featured by higher Ti and HREE concentrations and lower U/Yb ratios, reflecting hotter, drier magmas in juvenile rift and plume environments and cooler and wetter magmas in subduction environments (Fig. 12a–c). The mean calculated growth temperature of the late Mesoarchean magmatic zircons from the Bengbu and Jiaobei areas are 699 °C (6.52 ppm) and 678 °C (4.96 ppm; Liu *et al.* 2013*b*;

https://doi.org/10.1017/S0016756818000869 Published online by Cambridge University Press

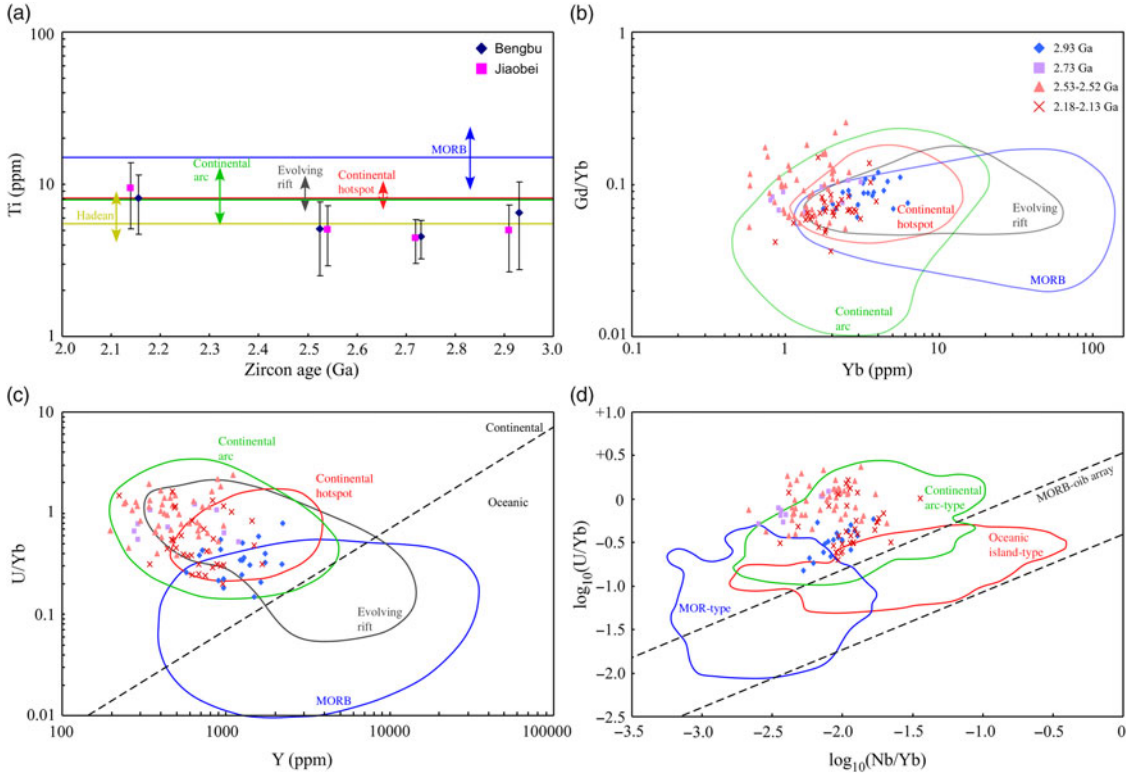

Fig. 12. (Colour online) (a) Comparison of Ti-in-zircon distributions of global zircon populations in different tectonic settings. Arrow represents middle 50% of zircon compositions for each population and line represents the median composition of the population (Carley *et al.* 2014). (b) Plots of Gd/Yb v. Yb (ppm) of zircons from different tectonic setting (Carley *et al.* 2014). (c) Plots of U/Yb v. Y (ppm) of zircons from different tectonic setting (Carley *et al.* 2014). Dashed lines delineate continental (above the line) and oceanic (MORB) compositional fields. (d) Density distribution plots based on geochemical proxies for tectonomagmatic setting; the contours shown are for 95% level (Grimes *et al.* 2015). MOR – mid-ocean ridge; MORB – mid-ocean-ridge basalt; OIB – ocean-island basalt.

Fig. 12a), respectively. Based on the similar rock type, SiO_2 and TiO_2 concentrations (Jahn *et al.* 2008; Wu *et al.* 2014*b*), which are similar to the Hadean zircons, are slightly lower than those of continental arc zircons (8 ppm; Fig. 12a) and much lower than those of MORB zircons (15 ppm; Carley *et al.* 2014; Fig. 12a). Due to the lack of reliable evidence to constrain a_{TiO2} and a_{SiO2}, we assumed them to be unity and obtained minimum zircon growth temperatures (Ferry & Watson, 2007), so the much lower temperatures of these late Mesoarchean zircons compared with MORB zircons are possibly due to an overestimation of a_{TiO2}. In addition, although zircon U/Yb ratios of the Bengbu (0.34) and Jiaobei areas (0.51; Liu *et al.* 2013*b*) show moderate differences, both are much higher than those of MORB zircons (0.06) and slightly lower than the Hadean zircons (0.60; Fig. 12c). Similar to the conclusion about the Hadean zircons proposed by Carley *et al.* (2014), we also suggest that the late Mesoarchean zircons in the southeastern NCC may reflect wetter and possibly cooler magmatism than Phanerozoic arcs.

5.b.3. Early Neoarchean

The granitoid gneisses of age *c.* 2.7 Ga in the Jiaobei Terrane display near to zero whole-rock $\varepsilon_{Nd}(t)$ values and zircon $\varepsilon_{Hf}(t)$ values and model ages of 2.9–3.0 Ga (Jahn *et al.* 2008; Liu *et al.* 2013*b*; Wu *et al.* 2014*b*; Xie *et al.* 2015). In combination with co-occurrences of low-HREE and high-HREE types, it is therefore suggested that the magmas were generated under different melting conditions during the same large-scale tectonic event, and the delaminated Mesoarchean lowest eclogite-facies crust was replaced by rising hot asthenospheric mantle which heated the residual Mesoarchean basaltic and intermediate lower crustal rocks (Jahn *et al.* 2008; Wu *et al.* 2014*b*; Xie *et al.* 2015). The continental hotspot setting for the early Neoarchean magmatic event does not contradict zircon trace element features (Fig. 12). U/Yb ratios (1.00±0.55 for Jiaobei and 0.96±0.42 for Bengbu; Liu *et al.* 2013*b*) and Yb/Gd ratios (21.0±7.5 for Jiaobei and 12.5±2.2 for Bengbu; Liu *et al.* 2013*b*) are all consistent with or slightly higher than those of the continental hotspot (0.66 and 12; Carley *et al.* 2014; Fig. 12b, c); the obviously lower Ti contents (4.43 ppm for Jiaobei and 4.53 ppm for Bengbu compared with 8 ppm for the continental hotspot) may imply a cooler asthenospheric mantle during the early Neoarchean Era (Fig. 12a), assuming a_{TiO2} and a_{SiO2} to be unity. On the other hand, in consideration of the similar 2.9–3.0 Ga crust growth event reflected by the Hf model ages of the early Neoarchean magmatic zircons in the Huoqiu, Bengbu and Jiaobei areas, which are much older than 2.7–2.8 Ga in other areas of the NCC (Wan *et al.* 2017), we suggest that the separated micro-block in the southern NCC did not unite with other parts of the NCC during the early Neoarchean Era.

5.b.4. Late Neoarchean – late Palaeoproterozoic

The late Neoarchean tectonic setting of the Eastern Block in the NCC has been under debate for a long time; one theory is that of a continental magmatic arc model (Peng *et al.* 2015; Wang *et al.* 2012*b*, 2015, 2017*b*; Nutman *et al.* 2011), whereas others prefer a mantle plume model (Geng *et al.* 2006; Yang *et al.* 2008; Wu *et al.* 2014*b*). In the Jiaobei Terrane, Wu et al. (2014*b*) suggested partial melting of pre-existing thickened lower crust with minor mantle-derived juvenile materials induced by a mantle plume, based on the high-HREE-type TTG, the large range of whole-rock $\varepsilon_{Nd}(t)$ values

https://doi.org/10.1017/S0016756818000869 Published online by Cambridge University Press

of −1.4 to +4.5 and zircon $\varepsilon_{Hf}(t)$ values of +1.3 to +7.6, and bimodal volcanic assemblages. However, Shan et al. (2015) proposed partial melting of subducted oceanic slab in a continental arc environment, mainly in consideration of the high Cr and Ni contents of TTG gneisses. For the zircon trace-element features, the Bengbu (5.10±2.58 ppm) and Jiaobei (5.04±2.14 ppm) areas have similar Ti contents which are much lower than those of Phanerozoic continental arc and continental hotspot (8 ppm; Carley *et al.* 2014; Fig. 12a). On the other hand, in consideration of the high U/Yb ratios of 1.05±0.46 for the Bengbu zircons (Fig. 12c), low Yb content (145±53 ppm; Fig. 12b) and low Yb/Gd ratios (11.3±4.2; Fig. 12b), slightly younger 2.49–2.52 Ga metamorphism, and Nb–Ta–Ti negative anomalies for the plagioclase amphibolite in the Jiagou xenoliths of age *c.* 2.5 Ga (Liu *et al.* 2013*a*), a late Neoarchean subduction-related setting at the southeastern North China Craton is more likely (Fig. 12d).

In the Bengbu area, the middle Palaeoproterozoic meta-mafic rocks from the Wuhe Group have zircon $\varepsilon_{Hf}(t)$ values of −6.22 to +8.38; their geochemical isotopic features are indicative of partial melting of sub-arc depleted mantle wedge modified by different degrees of slab-derived melts at an active continental margin (Liu *et al.* 2018). On the other hand, the coeval granites are characterized by high Zr, Nb, Ga and Y contents, TFeO/MgO ratios and Zr-saturation temperatures of over 850 °C, suggestive of an affinity with A-type granite (Yang *et al.* 2009; Wang *et al.* 2017*a*). The much higher whole-rock Zr-saturation temperatures (>850 °C) compared with the zircon growth temperature (727±44 °C) can be explained by the assumption of unity of a_{TiO2} and a_{SiO2}, so the calculated zircon crystallization temperatures are minimum estimates (Ferry & Watson, 2007). In the Jiaobei Terrane, *c.* 2.1 Ga hornblende-bearing monzogranitic gneiss and biotite-bearing monzogranitic gneiss (Liu *et al.* 2014) have also been reported. In the Liaoji area, voluminous middle Palaeoproterozoic A-type granitoids and meta-mafic rocks with arc-like geochemical features have been widely identified (Hao *et al.* 2004; Lu *et al.* 2004; Li & Zhao, 2007; Li & Chen, 2014; Meng *et al.* 2014; Yuan *et al.* 2015; Xu *et al.* 2017). These magmatic events at *c.* 2.2–2.0 Ga spatially constitute a linear Palaeoproterozoic magmatic belt along the JLJB, and their zircon Hf isotopic analyses indicate remelting of Neoarchean or older continental crustal (Liu *et al.* 2014, 2018; Wang *et al.* 2017*a*). In addition, the almost identical metamorphic ages of 1.84–1.88 Ga from the Huoqiu and Bengbu areas (Xu *et al.* 2006; Guo & Li, 2009; Liu *et al.* 2009, 2017*c*, 2018; Wan *et al.* 2010; Wang *et al.* 2013) implies that they have been involved in subduction- and collision-related tectonic processes at 1.9–1.8 Ga, similar to the Jiaobei Terrane (Zhou *et al.* 2008*b*; Wang *et al.* 2010; Tam *et al.* 2011; Liu *et al.* 2012*a*, 2017*d*). The potassic granites of age *c.* 2.1 Ga, consistent with A-type granite affinity, the meta-mafic rocks of age *c.* 2.1 Ga with arc-like geochemical features, and the subduction- and collision-related granulite-facies metamorphism of age 1.8–1.9 Ga in the Huoqiu, Bengbu and Jiaobei areas suggest that they are the southern extension of the JLJB.

6. Conclusions

New zircon U–Pb and Lu–Hf isotopes and trace-element compositions provided by this study for the (gneissic) granitoids of the Bengbu area in the southeastern NCC, together with the results of previous studies, lead to the following conclusions.

(1) U–Pb age data for magmatic zircons reveal that the Bengbu and Huoqiu areas underwent four felsic magmatism events at *c.* 2.93 Ga, 2.76–2.71 Ga, 2.56–2.52 Ga and 2.18–2.10 Ga, as well as mafic magmatism events at 2.71 Ga, 2.55 Ga and 2.13 Ga.
(2) Metamorphic zircon ages suggest that the Bengbu and Huoqiu areas experienced a regional metamorphic event at 2.52–2.48 Ga as for most other metamorphic complexes in the Eastern Block, and a Palaeoproterozoic tectonothermal event at 1.88–1.80 Ga, which was likely associated with the formation of the Jiao-Liao-Ji Belt.
(3) Xenocrystic, magmatic and metamorphic zircon U–Pb and Lu–Hf data indicate the presence of a Palaeoarchean–Mesoarchean micro-continent entrained in the Jiao-Liao-Ji Belt at the southeastern North China Craton.

Supplementary material. To view supplementary material for this article, please visit https://doi.org/10.1017/S0016756818000869.

Acknowledgements. We thank Liang Li for his laboratory assistance. We are also grateful for thoughtful and constructive reviews that significantly improved the quality of this paper. This research was funded by NSFC grants (nos 41430210 and 41622203).

References

ABGMR (1987) *Regional Geology of Anhui Province*. Beijing: Geological Publishing House, pp. 10–13 (in Chinese with English abstract).

Amelin Y, Lee DC and Halliday AN (2000) Early-middle Archaean crustal evolution deduced from Lu-Hf and U-Pb isotopic studies of single zircon grains. *Geochimica et Cosmochimica Acta* **64**, 4205–25.

Amelin Y, Lee DC, Halliday AN and Pidgeon RT (1999) Nature of the Earth's earliest crust from hafnium isotopes in single detrital zircons. *Nature* **399**, 252–55.

Anderson T (2002) Correction of common lead in U-Pb analyses that do not report ^{204}Pb. *Chemical Geology* **192**, 59–79.

Bai J and Dai FY (1996) The early Precambrian crustal evolution of China. *Journal of Southeast Asian Earth Sciences* **13**, 205–14.

Barker F (1979) Trondhjemite: definition, environment and hypotheses of origin. In *Trondhjemites, Dacites and Related Rocks* (ed F Barker), pp. 1–12. Amsterdam: Elsevier.

Barth AP, Wooden JL, Jacobson CE and Economos RC (2013) Detrital zircon as a proxy for tracking the magmatic arc system: the California arc example. *Geology* **41**, 223–26.

Bell EA, Harrison TM, Kohl IE and Young ED (2014) Eoarchean crustal evolution of the Jack Hills zircon source and loss of Hadean crust. *Geochimica et Cosmochimica* **146**, 27–42.

Blichert-Toft J and Albarede F (1997) The Lu-Hf geochemistry of chondrites and the evolution of the mantle-crust system. *Earth and Planetary Science Letters* **148**, 243–58.

Carley TL, Miller CF, Wooden JL, Padilla AJ, Schmitt AK, Economos RC, Binderman IN and Jordan BT (2014) Iceland is not a magmatic analog for the Hadean: evidence from the zircon record. *Earth and Planetary Science Letters* **405**, 85–97.

Corfu F, Hanchar JM, Hoskin PWO and Kinny P (2003) Atlas of zircon textures. In *Zircon, Reviews Mineralogy and Geochemistry*, vol. **53** (eds JM Hanchar and PWO Hoskin), pp. 468–500. Mineralogical Society of America.

Diwu CR, Sun Y, Wilde SA, Wang H, Dong Z, Zhang H and Wang Q (2013) New evidence for ca. 4.45 Ga terrestrial crust from zircon xenocrysts in Ordovician ignimbrite in the North Qinling Orogenic Belt, China. *Gondwana Research* **23**, 1484–90.

Dong CY, Wan YS, Xie HQ, Nutman AP, Xie SW, Liu SJ, Ma MZ and Liu DY (2017) The Mesoarchean Tiejiashan-Gongchangling potassic granite in the Anshan-Benxi area, North China Craton: origin by recycling of Paleo- to Eoarchean crust from U-Pb-Nd-Hf-O isotopic studies. *Lithos* **290**, 116–35.

Faure M, Lin W, Monie P, Breton NL, Poussineau S, Panis D and Deloule E (2003) Exhumation tectonics of the ultrahighpressure metamorphic rocks in

the Qinling orogen in east China: new petrological-structural-radiometric insights from the Shandong Peninsula. *Tectonics* **22**, 1018–40.

Faure M, Trap P, Lin W, Monie P and Bruguier O (2007) Polyorogenic evolution of the Paleoproterozoic Trans-North China Belt, new insights from the Lüliangshan-Hengshan-Wutaishan and Fuping massifs. *Episodes* **30**, 1–12.

Ferry JM and Watson EB (2007) New thermodynamic models and revised calibrations for the Ti-in-zircon and Zr-in-rutile thermometers. *Contributions to Mineralogy and Petrology* **154**, 429–37.

Ge WC, Zhao GC, Sun DY, Wu FY and Lin Q (2003) Metamorphic P-T path of the Southern Jilin complex: implications for tectonic evolution of the Eastern Block of the North China craton. *International Geology Review* **45**, 1029–43.

Geng YS, Liu FL and Yang CH (2006) Magmatic event at the end of the Archean in eastern Hebei Province and its geological implication. *Acta Geologica Sinica* **80**, 819–33.

Gerdes A and Zeh A (2009) Zircon formation versus zircon alteration-new insights from combined U-Pb and Lu-Hf in-situ LA-ICP-MS analyses, and consequences for the interpretation of Archean zircon from the Central Zone of the Limpopo Belt. *Chemical Geology* **261**, 230–43.

Griffin WL, Belousova EA, Shee SR, Pearson NJ and O'Reilly SY (2004) Archean crustal evolution in the northern Yilgarn Craton: U-Pb and Hf-isotope evidence from detrital zircons. *Precambrian Research* **131**, 231–82.

Grimes CB, John BE, Kelemen PB, Mazdab FK, Wooden JL, Cheadle MJ, Hanghøj K and Schwartz JJ (2007) Trace element chemistry of zircons from oceanic crust: a method for distinguishing detrital zircon provenance. *Geology* **35**, 643–46.

Grimes CB, Wooden JL, Cheadle MJ and John BE (2015) "Fingerprinting" tectono-magmatic provenance using trace elements in igneous zircon. *Contributions to Mineralogy and Petrology* **170**, 46.

Guo JH, O'Brien PJ and Zhai MG (2002) High-pressure granulites in the Sanggan area, North China craton: metamorphic evolution, P-T paths and geotectonic significance. *Journal of Metamorphic Geology* **20**, 741–56.

Guo SS and Li SG (2009) SHRIMP zircon U-Pb ages for the Paleoproterozoic metamorphic-magmatic events in the southeast margin of the North China Craton. *Science in China Series D: Earth Sciences* **52**, 1039–45 (in Chinese with English abstract).

Hao DF, Li SZ, Zhao GC, Sun M, Han ZZ and Zhao GT (2004) Origin and its constraint to tectonic evolution of Paleoproterozoic granitoids in the eastern Liaoning and Jilin Province, North China. *Acta Petrologica Sinica* **20**, 1409–16 (in Chinese with English abstract).

Harley SL, Kelly NM and Moller A (2007) Zircon behaviour and the thermal histories of mountain chains. *Elements* **3**, 25–30.

Harrison TM (2009) The Hadean crust: evidence from >4 Ga zircons. *Annual Review of Earth and Planetary Sciences* **37**, 479–505.

Hawkesworth CJ and Kemp AIS (2006) Using hafnium and oxygen isotopes in zircons to unravel the record of crustal evolution. *Chemical Geology* **226**, 144–62.

Heinonen A, Andersen T, Rämö OT and Whitehouse M (2015) The source of Proterozoic anorthosite and rapakivi granite magmatism: evidence from combined in situ Hf-O isotopes of zircon in the Ahvenisto complex, southeastern Finland. *Journal of the Geological Society* **172**, 103–12.

Hoskin PWO (2005) Trace-element composition of hydrothermal zircon and the alteration of Hadean zircon from the Jack Hills, Australia. *Geochimica et Cosmochimica Acta* **69**, 637–48.

Hoskin PWO and Black LP (2000) Metamorphic zircon formation by solid-state recrystallization of protolith igneous zircon. *Journal of Metamorphic Geology* **18**, 423–39.

Hoskin PWO and Schaltegger U (2003) The composition of zircon and igneous and metamorphic petrogenesis. *Reviews in Mineralogy and Geochemistry* **53**, 27–62.

Huang XL, Xu YG and Liu DY (2004) Geochronology, petrology and geochemistry of the granulite xenoliths from Nushan, east China: implication for a heterogeneous lower crust beneath the Sino-Korean Craton. *Geochimica et Cosmochimica Acta* **68**, 127–49.

Jahn BM, Liu DY, Wan YS, Song B and Wu JS (2008) Archean crustal evolution of the Jiaodong Peninsula, China, as revealed by zircon SHRIMP geochronology, elemental and Nd-isotope geochemistry. *American Journal of Science* **308**, 232–69.

Ji ZY (1993) New data on isotope age of the Proterozoic metamorphism rocks from northern Jiaodong and its geological significance. *Shandong Geology* **9**, 40–51 (in Chinese with English abstract).

Kamber BS (2015) The evolving nature of terrestrial crust from the Hadean, through the Archaean, into the Proterozoic. *Precambrian Research* **258**, 48–82.

Kenny GG, Whitehouse MJ and Kamber BS (2016) Differentiated impact melt sheets may be a potential source of Hadean detrital zircon. *Geology* **66**, 435–38.

Kinny PD and Maas R (2003) Lu-Hf and Sm-Nd isotope systems in Zircon. In *Zircon Reviews in Mineralogy and Geochemistry* vol. **53** (eds JM Hanchar and PWO Hoskin), pp. 327–41. Washington, DC: Mineralogical Society of America.

Kirkland CL, Smithies RH, Taylor RJM, Evans N and McDonald B (2015) Zircon Th/U ratios in magmatic environs. *Lithos* **212**, 397–414.

Kusky TM and Li JH (2003) Paleoproterozoic tectonic evolution of the North China Craton. *Journal of Asian Earth Sciences* **22**, 383–97.

Kusky TM, Li JH and Santosh M (2007) The Paleoproterozoic North Hebei Orogen: North China Craton's collisional suture with the Columbia supercontinent. *Gondwana Research* **12**, 4–28.

Li SZ and Zhao G (2007) SHRIMP U-Pb zircon geochronology of the Liaoji granitoids: constraints on the evolution of the Paleoproterozoic Jiao-Liao-Ji belt in the Eastern Block of the North China Craton. *Precambrian Research* **158**, 1–16.

Li SZ, Zhao GC, Sun M, Han ZZ, Hao DF, Luo Y and Xia XP (2005) Deformation history of the Paleoproterozoic Liaohe Group in the Eastern Block of the North China Craton. *Journal of Asian Earth Sciences* **24**, 659–74.

Li Z and Chen B (2014) Geochronology and geochemistry of the Paleoproterozoic meta-basalts from the Jiao-Liao-Ji Belt, North China Craton: implications for petrogenesis and tectonic setting. *Precambrian Research* **255**, 653–67.

Liu CH and Cai J (2017) Provenance and depositional age of the Baiyunshan Formation of the Fengyang Group in the Wuhe Complex: constraints from zircon U-Pb age and Lu-Hf isotopic studies. *Acta Petrologica Sinica* **33**, 2867–80 (in Chinese with English abstract).

Liu CH, Zhao GC, Liu FL and Cai J (2018) The southwestern extension of the Jiao-Liao-Ji belt in the North China Craton: geochronological and geochemical evidence from the Wuhe Group in the Bengbu area. *Lithos* **304**, 258–79, 10.1016/j.lithos.2018.01.021.

Liu DY, Nutman AP, Compston W, Wu JS and Shen QH (1992) Remnants of ≥3800 Ma crust in the Chinese part of the Sino-Korean craton. *Geology* **20**, 339–42.

Liu FL, Liu CH, Itano K, Iizuka T, Cai J and Wang F (2017b) Geochemistry, U-Pb dating, and Lu-Hf isotopes of zircon and monazite of porphyritic granites within the Jiao-Liao-Ji orogenic belt: implications for petrogenesis and tectonic setting. *Precambrian Research* **300**, 78–106.

Liu FL, Liu PH, Wang F, Liu CH and Cai J (2015b) Progresses and overviews of voluminous meta-sedimentary series within the Paleoproterozoic Jiao-Liao-Ji orogenic/mobile belt, North China Craton. *Acta Petrologica Sinica* **31**, 2816–46 (in Chinese with English abstract).

Liu FL, Robinson PT, Gerdes A, Xue HM, Liu PH and Liou JG (2010a) Zircon U-Pb ages, REE concentrations and Hf isotope composition of granitic leucosome and pegmatite from the north Sulu UHP terrane in China: constraints on the timing and nature of partial melting. *Lithos* **117**, 247–68.

Liu JH, Liu FL, Ding ZJ, Liu CH, Yang H., Liu PH, Wang F and Meng E (2013b) The growth, reworking and metamorphism of early Precambrian crust in the Jiaobei terrane, the North China Craton: constraints from U-Th-Pb and Lu-Hf isotopic systematics, and REE concentrations of zircon from Archean granitoid gneisses. *Precambrian Research* **224**, 287–303.

Liu JH, Liu FL, Ding ZJ, Liu PH, Guo CL and Wang F (2014) Geochronology, petrogenesis and tectonic implications of Paleoproterozoic granitoid rocks in the Jiaobei Terrane, North China Craton. *Precambrian Research* **255**, 685–98.

Liu JH, Liu FL, Ding ZJ, Yang H, Liu CH, Liu PH, Xiao LL, Zhao L and Geng J (2013d) U-Pb dating and Hf isotope study of detrital zircons from the Zhifu Group, Jiaobei Terrane, North China Craton: provenance and implications

https://doi.org/10.1017/S0016756818000869 Published online by Cambridge University Press

for Precambrian crustal growth and recycling. *Precambrian Research* **235**, 230–250.

Liu L and Yang XY (2015) Temporal, environmental and tectonic significance of the Huoqiu BIF, southeastern North China Craton: geochemical and geochronological constraints. *Precambrian Research* **261**, 217–33.

Liu L, Yang XY, Santosh M and Aulbach S (2015a) Neoarchean to Paleoproterozoic continental growth in the southeastern margin of the North China Craton: geochemical, zircon U-Pb and Hf isotope evidence from the Huoqiu complex. *Gondwana Research* **28**, 1002–18.

Liu L, Yang XY, Santosh M, Zhao GC and Aulbach S (2016) U-Pb age and Hf isotopes of detrital zircons from the Southeastern North China Craton: Meso-to Neoarchean episodic crustal growth in a shifting tectonic regime. *Gondwana Research* **35**, 1–14.

Liu PH, Liu FL, Cai J, Wang F, Liu CH, Liu JH, Yang H, Shi JR and Liu LS (2017d) Discovery and geological significance of high-pressure mafic granulites in the Pingdu-Anqiu area of the Jiaobei Terrane, the Jiao-Liao-Ji Belt, the North China Craton. *Precambrian Research* **303**, 445–69.

Liu PH, Liu FL, Liu CH, Wang F, Liu JH, Yang H, Cai J and Shi JR (2013c) Petrogenesis, P-T-t path, and tectonic significance of high-pressure mafic granulites from the Jiaobei terrane, North China Craton. *Precambrian Research* **233**, 237–58.

Liu PH, Liu FL, Yang H, Wang F and Liu JH (2012a) Protolith ages and timing of peak and retrograde metamorphism of the high-pressure granulites in the Shandong Peninsula, eastern North China Craton. *Geoscience Frontiers* **3**, 923–43.

Liu SW, Santosh M, Wang W, Bai X and Yang P (2011) Zircon U-Pb chronology of the Jianping Complex: implications for the Precambrian crustal evolution history of the northern margin of North China Craton. *Gondwana Research* **20**, 48–63.

Liu SW, Wang MJ, Wan YS, Guo RR, Wang W, Wang K, Guo BR, Fu JH and Hu FY (2017a) A reworked ca. 3.45 Ga continental microblock of the North China Craton: constraints from zircon U-Pb-Lu-Hf isotopic systematics of the Archean Beitai-Waitoushan migmatite-syenogranite complex. *Precambrian Research* **303**, 332–54.

Liu SW, Zhang J, Li QG, Zhang LF, Wang W and Yang PT (2012b) Geochemistry and U-Pb zircon ages of metamorphic volcanic rocks of the Paleoproterozoic Lüliang Complex and constraints on the evolution of the Trans-North China Orogen, North China Craton. *Precambrian Research* **222–223**, 173–90.

Liu YC, Wang AD, Li SG, Rolfo F, Li Y, Groppo C and Hou ZH (2013a) Composition and geochronology of the deep-seated xenoliths from the southeastern margin of the North China Craton. *Gondwana Research* **23**, 1021–39.

Liu YC, Wang AD, Rolfo F, Groppo C, Gu XF and Song B (2009) Geochronological and petrological constraints on Palaeoproterozoic granulite facies metamorphism in southeastern margin of the North China Craton. *Journal of Metamorphic Geology* **27**, 125–38.

Liu YC, Wang CC, Zhang PG, Groppo C, Rolfo F and Wang AD (2015c) Granulite facies metamorphism, partial melting and metasomatism in the Wuhe Complex at the southeastern margin of the North China Block. *Journal of Earth Sciences and Environment* **37**, 1–11 (in Chinese with English abstract).

Liu YC, Zhang PG, Wang CC, Groppo C, Rolfo F, Yang Y, Li Y, Deng LP and Song B (2017c) Petrology, geochemistry and zirconology of impure calcite marbles from the Precambrian metamorphic basement at the southeastern margin of the North China Craton. *Lithos* **290**, 189–209.

Liu YS, Gao S, Hu ZC, Gao CG, Zong KQ and Wang DB (2010b) Continental and oceanic crust recycling-induced melt-peridotite interactions in the Trans-North China Orogen: U-Pb dating, Hf isotopes and trace elements in zircons from mantle xenoliths. *Journal of Petrology* **51**, 537–71.

Lu SN (1998) Geochronology and Sm-Nd Isotopic geochemistry of Precambrian crystalline basement in eastern Shandong Province. *Earth Science Frontiers* (China University of Geosciences Beijing) **5**, 275–83 (in Chinese with English abstract).

Lu SN, Zhao GC, Wang HC and Hao GJ (2008) Precambrian metamorphic basement and sedimentary cover of the North China Craton: a review. *Precambrian Research* **160**, 77–93.

Lu XP, Wu FY, Guo JH, Wilde SA, Yang JH, Liu XM and Zhang XO (2006) Zircon U-Pb geochronological constraints on the Paleoproterozoic crustal evolution of the Eastern block in the North China Craton. *Precambrian Research* **146**, 138–64.

Lu XP, Wu FY, Zhang YB, Zhao CB, Yang JH and Guo CL (2004) Emplacement age and tectonic setting of the Paleoproterozoic Liaoji granites in Tonghua area, southern Jilin province. *Acta Petrologica Sinica* **20**, 381–92 (in Chinese with English abstract).

Ludwig KR (2003) *User's Manual for Isoplot 3.00: A Geochronological Toolkit for Microsoft Excel, Special Publication 4a*. Berkeley, California: Berkeley Geochronology Center.

Luo Y, Sun M, Zhao GC, Li SZ, Ayers JC, Xia X and Zhang J (2008) A comparison of U-Pb and Hf isotopic compositions of detrital zircons from the North and South Liaohe Groups: constraints on the evolution of the Jiao-Liao-Ji Belt, North China Craton. *Precambrian Research* **163**, 279–306.

Luo Y, Sun M, Zhao GC, Li SZ, Xu P, Ye K and Xia X (2004) LA-ICP-MS U-Pb zircon ages of the Liaohe Group in the Eastern Block of the North China Craton: constraints on the evolution of the Jiao-Liao-Ji Belt. *Precambrian Research* **134**, 349–71.

Lv B, Zhai MG, Li TS and Peng P (2012) Zircon U-Pb ages and geochemistry of the Qinglong volcano-sedimentary rock series in Eastern Hebei: implication for 2500 Ma intra-continental rifting in the North China Craton. *Precambrian Research* **208–211**, 145–60.

Meng E, Liu FL, Liu PH, Liu CH and Yang H (2014) Petrogenesis and tectonic significance of Paleoproterozoic meta-mafic rocks from central Liaodong Peninsula, northeast China: evidence from zircon U-Pb dating and in situ Lu-Hf isotopes, and whole-rock geochemistry. *Precambrian Research* **247**, 92–109.

Morel MLA, Nebel O and Nebel-Jacobsen YJ (2008) Hafnium isotope characterization of the GJ-1 zircon reference material by solution and laser ablation MC-ICPMS. *Chemical Geology* **255**, 231–35.

Mukherjee S, Dey A, Sanyal S, Ibanez-Mejia M, Dutta U and Sengupta P (2017) Petrology and U-Pb geochronology of zircon in a suite of charnockitic gneisses from parts of the Chotanagpur Granite Gneiss Complex (CGGC): evidence for the reworking of a Mesoproterozoic basement during the formation of the Rodinia supercontinent. In *Crustal Evolution of India and Antarctica: The Supercontinent Connection* (eds NC Pant and S Dasgupta), pp. 197–231. *Geological Society of London, Special Publication no.* 457.

Nutman AP, Wan YS, Du LL, Friend CRL, Dong CY, Xie HQ, Wang W, Sun HY and Liu DY (2011) Multistage late Neoarchaean crustal evolution of the North China Craton, eastern Hebei. *Precambrian Research* **189**, 43–65.

Paulsen T, Deering C, Sliwinski J, Bachmann O and Guillong M (2016) A continental arc tempo discovered in the Pacific-Gondwana margin mudpile? *Geology* **44**, 915–18.

Peng P, Wang C, Wang XP and Yang SY (2015) Qingyuan high-grade granite greenstone terrain in the Eastern North China Craton: root of a Neoarchaean arc. *Tectonophysics* **662**, 7–21.

Qian JH and Wei CJ (2016) P-T-t, evolution of garnet amphibolites in the Wutai- Hengshan area, north china craton: insights from phase equilibria and geochronology. *Journal of Metamorphic Geology* **34**, 423–46.

Santosh M (2010) Assembling North China Craton within the Columbia supercontinent: the role of double-sided subduction. *Precambrian Research* **178**, 149–67.

SBGMR (1991) *Regional Geology of Shandong Province*. Beijing, China: Geological Publishing House, pp. 6–52 (in Chinese with English abstract).

Shan HX, Zhai MG, Wang F, Zhou YY, Santosh M, Zhu XY, Zhang HF and Wang W (2015) Zircon U-Pb ages, geochemistry, and Nd–Hf isotopes of the TTG gneisses from the Jiaobei terrane: implications for Neoarchean crustal evolution in the North China Craton. *Journal of Asian Earth Sciences* **98**, 61–74.

Song B, Nutman AP, Liu DY and Wu JS (1996) 3800 to 2500 Ma crust in the Anshan area of Liaoning Province, northeastern China. *Precambrian Research* **78**, 79–94.

Sun SS and McDonough WF (1989) Chemical and isotopic systematics of oceanic basalts: implications for mantle composition and processes. In *Magmatism in the Ocean Basins* (eds AD Saunders and MJ Norry), pp. 313–45. Geological Society of London, Special Publication no. 42.

https://doi.org/10.1017/S0016756818000869 Published online by Cambridge University Press

Tam PY, Zhao GC, Liu FL, Zhou XW, Sun M and Li SZ (2011) Timing of metamorphism in the Paleoproterozoic Jiao-Liao-Ji Belt: new SHRIMP U-Pb zircon dating of granulites, gneisses and marbles of the Jiaobei massif in the North China Craton. *Gondwana Research* **19**, 150–62.

Tang J, Zheng YF, Wu YB, Gong B and Liu XM (2007) Geochronology and geochemistry of metamorphic rocks in the Jiaobei terrane: constraints on its tectonic affinity in the Sulu orogen. *Precambrian Research* **152**, 48–82.

Tang J, Zheng YF, Wu YB, Zha XP and Zhou JB (2004) Zircon U-Pb ages and oxygen isotopes of metamorphic rocks in the western part of the Shandong Peninsula. *Acta Petrologic Sinica* **20**, 1063–86 (in Chinese with English abstract).

Tu YJ, Chen CT and Tang LG (1992) The classification and structural features of the Precambrian metamorphic rock series in the northern part of the Jianghuai region. *Regional Geology of China* **3**, 248–56 (in Chinese with English abstract).

Wallis S, Enami M and Banno S (1999) The Sulu UHP Terrane: a review of the petrology and structural geology. *International Geology Review* **41**, 906–20.

Wan YS, Dong CY, Liu DY, Kröner A, Yang CH, Wang W, Du LL, Xie HQ and Ma MZ (2012) Zircon ages and geochemistry of late Neoarchean syenogranites in the North China Craton: a review. *Precambrian Research* **222–223**, 265–89.

Wan YS, Dong CY, Ren P, Bai WQ, Xie HQ, Xie SW and Liu DY (2017) Spatial and temporal distribution, compositional characteristics and formation and evolution of Archean TTG rocks in the North China Craton: a synthesis. *Acta Ptrologica Sinica* **33**, 1405–19 (in Chinese with English abstract).

Wan YS, Dong CY, Wang W, Xie HQ and Liu DY (2010) Archean basement and a Paleoproterozoic Collision Orogen in the Huoqiu Area at the Southeastern Margin of North China Craton: evidence from sensitive high resolution ion micro-probe U-Pb zircon geochronology. *Acta Geologica Sinica* **84**, 91–104.

Wan YS, Liu DY, Dong CY, Xie HQ, Kröner A, Ma MZ, Liu SJ, Xie SW and Ren P (2015) Formation and evolution of Archean continental crust of the North China Craton. In *Precambrian Geology of China* (ed. MG Zhai), pp. 59–136. Berlin, Heidelberg: Springer.

Wan YS, Liu DY, Song B, Wu JS, Yang CH, Zhang ZQ and Geng YS (2005) Geochemical and Nd isotopic compositions of 3.8 Ga meta-quartz dioritic and trondhjemitic rocks from the Anshan area and their geological significance. *Journal of Asian Earth Sciences* **4**, 563–75.

Wan YS, Song B, Liu DY, Wilde SA, Wu JS, Shi YR, Yin XY and Zhou HY (2006) SHRIMP U-Pb zircon geochronology of Paleoproterozoic metasedimentary rocks in the North China Craton: evidence for a major Late Palaeoproterozoic tectonothermal event. *Precambrian Research* **149**, 249–71.

Wan YS, Xie SW, Yang CH, Kröner A, Ma MZ, Dong CY, Du LL, Xie HQ and Liu DY (2014) Early Neoarchean (ca. 2.7 Ga) tectono-thermal events in the North China Craton: a synthesis. *Precambrian Research* **247**, 45–63.

Wan YS, Xu ZY, Dong CY, Nutman A, Ma MZ, Xie HQ, Liu SJ, Liu DY, Wang HC and Cu H (2013) Episodic Paleoproterozoic (ca. 2.45, ca. 1.95 and ca. 1.85 Ga) mafic magmatism and associated high temperature metamorphism in the Daqingshan area, North China Craton: SHRIMP zircon U-Pb dating and whole rock geochemistry. *Precambrian Research* **224**, 71–93.

Wang AD, Liu YC, Gu XF, Hou ZH and Song B (2012a) Late-Neoarchean magmatism and metamorphism at the southeastern margin of the North China Craton and their tectonic implications. *Precambrian Research* **220**, 65–79.

Wang AD, Liu YC, Santosh M and Gu XF (2013) Zircon U-Pb geochronology, geochemistry and Sr-Nd-Pb isotopes from the metamorphic basement in the Wuhe Complex: implications for Neoarchean active continental margin along the southeastern North China Craton and constraints on the petrogenesis of Mesozoic granitoids. *Geoscience Frontiers* **4**, 57–71.

Wang CC, Liu YC, Zhang PG, Zhao GC, Wang AD and Song B (2017a) Zircon U-Pb geochronology and geochemistry of two types of Paleoproterozoic granitoids from the southeastern margin of the North China Craton: constraints on petrogenesis and tectonic significance. *Precambrian Research* **303**, 268–90.

Wang F, Liu FL, Liu PH and Liu JH (2010) Metamorphic evolution of Early Precambrian khondalite series in North Shandong Province. *Acta Petrolgica Sinica* **26**, 2057–72 (in Chinese with English abstract).

Wang QY, Zheng JP, Pan YM, Dong YJ, Liao FX, Zhang Y, Zhang L, Zhao G and Tu ZB (2014a) Archean crustal evolution in the southeastern North China Craton: new data from the Huoqiu Complex. *Precambrian Research* **255**, 294–315.

Wang W, Liu SW, Cawood PA, Guo RR, Bai X and Guo BR (2017b) Late Neoarchean crust-mantle geodynamics: evidence from Pingquan complex of the northern Hebei Province, North China Craton. *Precambrian Research* **303**, 470–93.

Wang W, Liu SW, Santosh M, Wang G, Bai X and Guo R (2015) Neoarchean intraoceanic arc system in the Western Liaoning Province: implications for Early Precambrian crustal evolution in the Eastern Block of the North China Craton. *Earth-Science Reviews* **150**, 329–64.

Wang W, Liu SW, Wilde SA, Li QG, Zhang J, Xiang B, Yang PT and Guo RR (2012b) Petrogenesis and geochronology of Precambrian granitoid gneisses in Western Liaoning Province: constraints on Neoarchean to early Paleoproterozoic crustal evolution of the North China Craton. *Precambrian Research* **222–223**, 290–311.

Wang W, Zhai MG, Li TS, Santosh M, Zhao L and Wang HZ (2014b) Archean-Paleoproterozoic crustal evolution in the eastern North China Craton: zircon U-Th-Pb and Lu-Hf evidence from the Jiaobei terrane. *Precambrian Research* **241**, 146–60.

Wu FY, Li XH, Zheng YF and Gao S (2007) Lu-Hf isotopic systematics and their applications in petrology. *Acta Petrologica Sinica* **23**, 185–220 (in Chinese with English abstract).

Wu FY, Zhang YB, Yang JH, Xie LW and Yang YH (2008) Zircon U-Pb and Hf isotopic constraints on the Early Archean crustal evolution in Anshan of the North China Craton. *Precambrian Research* **167**, 339–62.

Wu JS, Geng YS and Shen QH (1998) *Archean Geology Characteristics and Tectonic Evolution of Sino-Korean Paleocontinent*. Beijing: Geological Publishing House, pp. 192–211 (in Chinese with English abstract).

Wu ML, Zhao GC, Sun M and Li SZ (2014b) A synthesis of geochemistry and Sm-Nd isotopes of Archean granitoid gneisses in the Jiaodong Terrane: constraints on petrogenesis and tectonic evolution of the Eastern Block, North China Craton. *Precambrian Research* **255**, 885–99.

Wu ML, Zhao GC, Sun M, Li SZ, Bao ZA, Tam PY, Eizenhöefer PR and He YH (2014a) Zircon U-Pb geochronology and Hf isotopes of major lithologies from the Jiaodong Terrane: implications for the crustal evolution of the Eastern Block of the North China Craton. *Lithos* **190**, 71–84.

Wu ML, Zhao GC, Sun M, Li SZ, He YH and Bao ZA (2013) Zircon U-Pb geochronology and Hf isotopes of major lithologies from the Yishui Terrane: implications for the crustal evolution of the Eastern Block, North China Craton. *Lithos* **170–171**, 164–78.

Xie HQ, Wan YS, Wang SJ, Liu DY, Xie SW, Liu SJ, Dong CY and Ma MZ (2013) Geology and zircon dating of trondhjemitic gneiss and amphibolite in the Tangezhuang area, eastern Shandong. *Acta Petrologica Sinica* **29**, 619–29 (in Chinese with English abstract).

Xie SW, Wang SJ, Xie HQ, Liu SJ, Dong CY, Ma MZ, Liu DY and Wan YS (2014b) SHRIMP U-Pb dating of detrital zircons from the Fenzishan Group in eastern Shandong, North China Craton. *Acta Petrologica Sinica* **30**, 2989–98 (in Chinese with English abstract).

Xie SW, Wang SJ, Xie HQ, Liu SJ, Dong CY, Ma MZ, Ren P and Liu DY (2015) Petrogenesis of ca. 2.7 Ga TTG rocks in the Jiaodong terranes, North China Craton and its geological implications. *Acta Petrologica Sinica* **31**, 2974–90 (in Chinese with English abstract).

Xie SW, Xie HQ, Wang SJ, Kröner A, Liu SJ, Zhou HY, Ma MZ, Dong CY, Liu DY and Wan YS (2014a) Ca. 2.9 Ga granitoid magmatism in eastern Shandong, North China Craton: zircon dating, Hf-in-zircon isotopic analysis and whole-rock geochemistry. *Precambrian Research* **255**, 538–62.

Xu W, Liu FL and Liu CH (2017) Petrogenesis and geochemical characteristics of the North Liaohe metabasic rocks, Jiao-Liao-Ji orogenic belt and their tectonic significance. *Acta Petrologica Sinica* **33**, 2743–57 (in Chinese with English abstract).

Xu WL, Gao S, Wang Q, Wang D and Liu Y (2006) Mesozoic crustal thickening of the eastern North China craton: evidence from eclogite xenoliths and petrologic implications. *Geology* **34**, 721–24.

Xu X, Hou MJ, Qiu RL, Wu LB and Li JS (2005) ^{40}Ar-^{39}Ar dating of granites and related dikes in the Bengbu area on the southeastern margin of the North China block. *Geology in China* **32**, 588–95 (in Chinese with English abstract).

Yang DB, Xu WL, Pei FP and Wang QH (2009) Petrogenesis of the Paleoproterozoic K-feldspar granites in Bengbu Uplift: constraints from

https://doi.org/10.1017/S0016756818000869 Published online by Cambridge University Press

petro-geochemistry, zircon U-Pb dating and Hf isotope. *Earth Science-Journal of China University of Geosciences* **34**, 148–64 (in Chinese with English abstract).

Yang JH, Wu FY, Wilde SA and Zhao GC (2008) Petrogenesis and geodynamics of Late Archean magmatism in eastern Hebei, eastern North China Craton: geochronological, geochemical and Nd-Hf isotopic evidence. *Precambrian Research* **167**, 125–49.

Yang XY, Wang BH, Du ZB, Wang QC, Wang YX, Tu ZB, Zhang WL and Sun WD (2012) On the metamorphism of the Huoqiu Group, formation ages and BIF forming mechanism of the Huoqiu iron deposit, South margin of the North China Craton. *Acta Petrologica Sinica* **28**, 3476–96 (in Chinese with English abstract).

Yin CQ, Zhao GC, Guo JH, Sun M, Xia XP, Zhou XW and Liu CH (2011) U-Pb and Hf isotopic study of zircons of the Helanshan Complex: constrains on the evolution of the Khondalite Belt in the Western Block of the North China Craton. *Lithos* **122**, 25–38.

Yin CQ, Zhao GC, Wei CJ, Sun M., Guo JH and Zhou XW (2014) Metamorphism and partial melting of high-pressure pelitic granulites from the Qianlishan Complex: constraints on the tectonic evolution of the Khondalite Belt in the North China Craton. *Precambrian Research* **242**, 172–86.

Yuan LL, Zhang XH, Xue FH, Han CM, Chen HH and Zhai MG (2015) Two episodes of Paleoproterozoic mafic intrusions from Liaoning province, North China Craton: petrogenesis and tectonic implications. *Precambrian Research* **264**, 119–39.

Zeh A, Gerdes A, Jay BJ and Klemd R (2010) U-Th-Pb and Lu-Hf systematics of zircon from TTG's, leucosomes, meta-anorthosites and quartzites of the Limpopo Belt (South Africa): constraints for the formation, recycling and metamorphism of Paleoarchean crust. *Precambrian Research* **179**, 50–68.

Zhai MG, Bian AG and Zhao TP (2000) The amalgamation of the supercontinent of North China Craton at the end of Neo-Archaean and its breakup during late Palaeoproterozoic and Mesoproterozoic. *Science in China (Series D-Earth Science)* **43**, 219–32.

Zhai MG, Guo JH and Liu WJ (2005) Neoarchean to Paleoproterozoic continental evolution and tectonic history of the North China craton. *Journal of Asian Earth Sciences* **24**, 547–61.

Zhai MG, Li TS, Peng P, Hu B, Liu F and Zhang YB (2010) Precambrian key tectonic events and evolution of the North China Craton. In *The Evolving Continents: Understanding Processes of Continental Growth* (eds TM Kusky, MG Zhai and WJ Xiao), pp. 235–62. Geological Society of London, Special Publication no. **338**.

Zhai MG and Peng P (2007) Paleoproterozoic events in North China Craton. *Acta Petrologica Sinica* **23**, 2665–82 (in Chinese with English abstract).

Zhai MG and Santosh M (2011) The early Precambrian odyssey of the North China Craton: a synoptic overview. *Gondwana Research* **20**, 6–25.

Zhang HF, Ying JF, Santosh M and Zhao GC (2012) Episodic growth of Precambrian lower crust beneath the North China Craton: a synthesis. *Precambrian Research* **222–223**, 255–264.

Zhang J, Zhao GC, Li SZ, Sun M, Liu SW and Yin CQ (2009) Deformational history of the Fuping Complex and new U-Th-Pb geochronological constraints: implications for the tectonic evolution of the Trans-North China Orogen. *Journal of Structural Geology* **31**, 177–93.

Zhang SB, Tang J and Zheng YF (2014) Contrasting Lu-Hf isotopes in zircon from Precambrian metamorphic rocks in the Jiaodong Peninsula: constraints on the tectonic suture between North China and South China. *Precambrian Research* **245**, 29–50.

Zhang YH, Wei CJ, Tian W and Zhou XW (2013) Reinterpretation of metamorphic age of the Hengshan Complex, North China Craton. *Chinese Science Bulletin* **58**, 4300–307.

Zhao GC, Cawood PA, Li SZ, Wilde SA, Sun M, Zhang J, He YH and Yin CQ (2012) Amalgamation of the North China Craton: key issues and discussion. *Precambrian Research* **222–223**, 55–76.

Zhao GC, Sun M, Wilde SA and Li SZ (2005) Late Archean to Paleoproterozoic evolution of the North China Craton: key issues revisited. *Precambrian Research* **136**, 177–202.

Zhao GC, Wilde S, Cawood P and Lu L (1998) Thermal evolution of Archean basement rocks from the Eastern part of the North China Craton and its bearing on tectonic setting. *International Geology Review* **40**, 706–21.

Zhao T, Zhu G, Lin SZ and Wang HQ (2016) Indentation-induced tearing of a subducting continent: evidence from the Tan-Lu Fault Zone, East China. *Earth-Science Reviews* **152**, 14–36.

Zheng YF, Zhao ZF, Wu YB, Zhang SB, Liu XM and Wu FY (2006) Zircon U-Pb age Hf and O isotope constraints on protolith origin of ultrahigh-pressure eclogite and gneiss in the Dabie orogen. *Chemical Geology* **231**, 135–58.

Zhou JB, Wilde SA, Zhao GC, Zhang XZ, Zheng CQ, Jin W and Cheng H (2008a) SHRIMP U-Pb zircon dating of the Wulian complex: defining the boundary between the North and South China Craton in the Sulu Orogenic Belt, China. *Precambrian Research* **162**, 559–76.

Zhou XW, Wei CJ, Geng YS and Zhang LF (2004) Discovery and implications of the high-pressure pelitic granulite from the Jiaobei massif. *Chinese Science Bulletin* **49**, 1942–48.

Zhou XW, Zhao GC, Wei CJ, Geng YS and Sun M (2008b) EPMA U-Th-Pb monazite and SHRIMP U-Pb zircon geochronology of high-pressure pelitic granulites in the Jiaobei massif of the North China Craton. *American Journal of Science* **308**, 328–50.

https://doi.org/10.1017/S0016756818000869 Published online by Cambridge University Press